Review

Emergence of Raman Spectroscopy as a Probing Tool for Theranostics

Ruchi Singh, Vikas Yadav, Ashish Kumar Dhillon, Arti Sharma, Tripti Ahuja, Soumik Siddhanta✉

Department of Chemistry, Indian Institute of Technology Delhi, Hauz Khas, New Delhi – 110016, India

*All the authors have contributed equally to this manuscript.

✉ Corresponding author: Dr. Soumik Siddhanta. soumik@iitd.ac.in

Abstract

Although medical advances have increased our grasp of the amazing morphological, genetic, and phenotypic diversity of diseases, there are still significant technological barriers to understanding their complex and dynamic character. Specifically, the complexities of the biological systems throw a diverse set of challenges in developing efficient theranostic tools and methodologies that can probe and treat pathologies. Among several emerging theranostic techniques such as photodynamic therapy, photothermal therapy, magnetic resonance imaging, and computed tomography, Raman spectroscopy (RS) is emerging as a promising tool that is a label-free, cost-effective, and non-destructive technique. It can also provide real-time diagnostic information and can employ multimodal probes for detection and therapy. These attributes make it a perfect candidate for the analytical counterpart of the existing theranostic probes. The use of biocompatible nanomaterials for the fabrication of Raman probes provides rich structural information about the biological molecules, cells, and tissues and highly sensitive information down to single-molecule levels when integrated with advanced RS tools. This review discusses the fundamentals of Raman spectroscopic tools such as surface-enhanced Raman spectroscopy and Resonance Raman spectroscopy, their variants, and the associated theranostic applications. Besides the advantages, the current limitations, and future challenges of using RS in disease diagnosis and therapy have also been discussed.

Keywords: Theranostics, plasmonic probes, Raman and surface-enhanced Raman spectroscopy, photothermal therapy, nanomedicine

Introduction

Theranostics is a combination of techniques involving diagnostic tests in conjunction with ad hoc medication. It relies on spectroscopic tools for diagnosis and has acquired importance in personalized medicine, particularly in curing fatal diseases [1]. Theranostic approaches have been primarily introduced and developed for early-stage detection and prevention of complex diseases that impose a significant economic and emotional burden on the patient population. According to the World Health Organization (WHO), cancer is a leading cause of death and a report by GLOBOCAN2020 indicates that the socioeconomic burden generated by cancer is expected to be shared by 28.4 million patients globally by 2040 [2, 3]. A diagnostic test combined with an appropriate therapy may allow clinicians to modify the treatment plan based on real-time diagnostic data, making it more suited to the patients being studied [4, 5]. Therefore, successful therapeutic and diagnostic management necessitates carefully selecting compatible theranostic methods.

Traditionally, fluorescent probes have been used widely in theranostics to probe living systems with better spatiotemporal resolution [6]. However, photobleaching, phototoxicity, and the presence of bulkier fluorescent moieties limit their use in spectroscopy and imaging [6]. Similarly, other existing techniques, such as computed tomography

(CT), photodynamic therapy (PDT), photothermal therapy (PTT), magnetic resonance imaging (MRI), *etc.*, can be modified and integrated with other suitable probes for theranostic applications. However, the photosensitizers employed in PDT, stay in the blood for a considerable amount of time and might cause phototoxicity when exposed to light. Similarly, the heat used in PDT can damage normal tissues, too, thus limiting their use [7]. Whereas, Raman spectroscopy (RS), an optical spectroscopy tool, provides a non-invasive way of studying biochemical and molecular processes without adversely affecting the biological system. RS is currently being explored in theranostics along with its non-linear and plasmon-enhanced counterparts [8, 9]. Compared to fluorescence and other bio-imaging methods, RS has a number of advantages, including the ability to use very stable molecular probes, a shorter spectrum bandwidth, a high signal-to-noise ratio, and does not require labels [10]. It has been used for the early diagnosis and treatment of various neurodegenerative diseases such as Alzheimer's and Parkinson's [11] [12]. Besides conventional tissue biopsies or investigations, RS has been utilized for four primary purposes. Firstly, it has a relatively high capability of predicting changes inside complex biomolecules and biological systems effectively. Since cell biochemistry is dynamic and constantly evolving, RS provides a practical approach to identifying the vibrational fingerprints of living cells in real-time. Using correlation spectra and chemometric techniques, it can also distinguish between diseased and normal tissues under *in vivo* and *in vitro* conditions [13] [14]. Secondly, the scattering cross-section of water is very low and does not interfere with the spectra of bioactive molecules in physiological conditions. The third salient point of RS is the ability to probe a wide range of samples with distinct physical states (bulk, surface, solid, liquid, particles), variable size ranges (from centimeters to nanometres), and various biological samples simultaneously. Finally, it can provide real-time biological information of discriminated cellular components and high-resolution imaging at a lower cost than other biomedical imaging techniques like ultrasound imaging and MRI. Moreover, RS can be coupled with nanoparticle-based therapeutic agents, making it a viable alternative to fluorescence spectroscopy in theranostics.

The efficiency of RS in probing deeper tissues and performing bio-imaging with high sensitivity has enabled it to be used for the early diagnosis of pathological conditions [2]. Some variants of RS include Surface-enhanced Raman spectroscopy (SERS), and Resonance Raman spectroscopy (RRS) [15-17]. These variants of RS are categorized as linear and non-linear processes. Coherent anti-Stokes Raman spectroscopy (CARS), a non-linear Raman microspectroscopic technique, has a better sensitivity than conventional RS. However, a non-resonant background in the CARS spectrum of biomolecules complicates the analysis and hinders accurate interpretation [15, 16, 18, 19]. Other techniques, such as spatially offset Raman spectroscopy (SORS), has the potential to probe living tissues through a depth of 5 cm, facilitating enhanced sensitivity up to 2 orders of magnitude in comparison to conventional RS [20][21]. The plasmon-enhanced counterpart, popularly known as SERS, is an effective tool for analyzing the vibrational characteristics of analytes at low concentrations upto single molecule levels [22] [23]. Moreover, its ability to identify unique fingerprint regions in individual cells and tissues makes it a promising diagnostic tool [24] [25]. It has been further employed to detect a variety of disease biomarkers including those of the Human Immune Virus (HIV), several types of cancer, and so on [26] [27].

Nanoparticles (NPs) are an integral part of theranostic-based drug delivery. The rational design of nano-probes and substrates is one of the critical factors for optimizing theranostic applications [28]. Some of the most efficient NP probes are magnetic NPs (MagNPs), plasmon-based gold and silver NPs, silica NPs, and polymeric NPs. Other options include nanocarbon materials and metal oxide NPs, which due to their ease of surface functionalization, have emerged as excellent probes for numerous biological applications [29], such as imaging [30], drug transport [31], and bio-sensing [32]. One of the best examples of carbon-based probes is the needle-shaped carbon nanotubes (CNTs) that allow enhanced drug loading with minimal or no effects on the cell penetration process [33-35]. Other classes of probes include SERS active nanoparticles and substrates such as metal film on nanoparticle (MFON) that function as an efficient and reproducible plasmonic substrate widely used in bioimaging, chemical sensing, bioanalysis, etc. [36-41]. Similarly, a class of NPs known as Janus NPs possesses multiple properties in the same particle. Due to their intrinsic anisotropy, they have attracted great interest in imaging, nanocarrier fabrication, cancer therapy, and theranostics [42]. In theranostic applications, where the photothermal application has been the preferred therapy, many morphologies of SERS probes, such as rods, spheres, nanostars, etc., have been employed. Therefore, the combination of NP-based probes destroys not only diseased cells using PTT or facilitates targeted drug release but also provides simultaneous diagnostic multimodal

information that can be achieved using Raman-based strategies [43, 44].

In this review, we have discussed the utilization of RS and its variants for theranostic applications. We have highlighted the fabrication strategies and applicability of different Raman probes such as plasmonic NPs, molecular probes, carbon-based nanomaterials, and metal oxide semiconductors for PTT, sensing, and bioimaging.

Principles of Raman Spectroscopy, its Variants, and their Preliminary Clinical Applications

RS is a non-destructive analytical tool that can examine various materials with exquisite molecular specificity [45]. It is an inelastic scattering process where electromagnetic radiation strikes the sample, leading to an increase or decrease in the energy of scattered light [46]. The inelastic scattering process is called Stokes scattering when the outgoing photon's energy is less than the incident photons, and anti-Stokes when the outgoing photon's energy is more than the incident one (**Figure 1A**) [47]. The difference between the incoming and inelastically scattered photon's energy is termed as "Raman shift." The main limitation of RS is that approximately one in 10^6 photons undergo inelastic scattering, which makes it a weak phenomenon. The following equation gives the Raman scattered intensity (I_R) in terms of the polarizability factor [48].

$$I_R = I_0 \nu^4 N \left(\frac{d\alpha}{dQ}\right)^2$$

Where I_o is the intensity of incident radiation and $\boldsymbol{\nu}$ is the frequency of the incoming radiation, N is the number of molecules scattered, and $d\alpha/dQ$ represents the change in polarization of the molecular vibrations. The advent of lasers and the development of optics have greatly improved the performance of Raman spectrometers allowing them to be used in biology and medicine. However, using laser excitation of higher power to achieve a good signal-to-noise ratio can increase the possibility of photodecomposition and degradation of the sample. Additionally, the scattered light can be accompanied by electronic excitations leading to fluorescence emission. This emission mostly interferes with the Raman signals and often appears as background noise in a biological system [49][50]. In comparison to other advance spectrometric techniques, Raman techniques such as RRS, Tip-enhanced Raman spectroscopy, and SERS enhance the weak Raman signals and reduce the fluorescence background [51-54]. One of the variants of RS suitable for applications in biology and medicine is SERS which was first discovered by

Fleischmann *et al.* [55] in 1974 where they observed the enhancement of Raman signals from pyridine molecules electrochemically adsorbed on the surface of the plasmonic silver nanoparticles (AgNPs) [56]. Later, Albrecht, Creighton, Jeanmarie, and van Duyne explained the reason for the signal enhancement in SERS, originating from strong electromagnetic fields at the metal surface (Jeanmaire and van Duyne) or by the formation of a molecule–metal complex (Creighton and Albrecht) [57] [58]. Thus, the SERS enhancement can be broadly classified as an electromagnetic enhancement (EME) or chemical enhancement (CE). **Electromagnetic enhancement (EME):** Such enhancement occurs due to the localization of the electromagnetic field on the surface of the NPs. The enhancement factor contributed by EME is strong and equivalent to 10^{10}-10^{12} times the total SERS enhancement. EME is independent of the type of molecule. In this enhancement, direct chemical contact of molecules with the plasmonic substrate is not required; however, the molecules should not be far from the substrate, i.e., the acceptable gap between a molecule and NP is 1-10 nm. Hence such enhancements are considered long-range effects. In EME, the spatial localized regions with high electric fields, termed hotspots, play an important role in the enhancement **Figure 1B** (bottom) [59]. In EME, two processes occur simultaneously, i.e., local field enhancement followed by re-radiation enhancement. The EME of a single molecule can be calculated using the below equation:

$$G_{SERS}^{Em}(E^4) = M_{Loc}^Z(\omega_L)M_{Loc}^Z(\omega_R)$$
$$= [\frac{E_{Loc\,(\omega_L)}}{E\,(\omega_L)}]^2 * [\frac{E_{Loc}\,\omega_R}{E\,\omega_R}]^2$$

Where, $G_{SERS}^{Em}(E^4)$ corresponds to electromagnetic enhancement factor, $M_{Loc}^Z(\omega_L)$ and $M_{Loc}^Z(\omega_R)$ are the field enhancements generated by a laser polarized along Z at the laser and at the Raman frequency, respectively, ω_L and ω_R attributes to laser and Raman angular frequencies, respectively.

Chemical Enhancement (CE): The formation of NP-molecule complexes results in chemical enhancement **Figure 1B** (top). CE contributes 10^2-10^3 orders of magnitude enhancement to total SERS and depends on the type of molecule involved in SERS. In CE, a direct interaction of the molecule with NPs is required; therefore, such enhancement is termed as a short-range effect. The CE can be defined using the below equation:

$$G_{SERS}^{Chem} = \frac{\sigma_k^{ads}}{\sigma_k^{free}}$$

Where G_{SERS}^{Chem} corresponds to the chemical

enhancement factor, σ_k^{ads} and σ_k^{free} attribute to the Raman cross-section of the adsorbed molecule and free molecule, respectively. Both the enhancement factors combine to give the total SERS enhancement factor. Moreover, the power of total SERS is equivalent to the product of SERS enhancement (EME and CE) and the scattered power of Raman (P_{Raman}). A detailed explanation of the mechanisms of SERS enhancement is given in the article of Roberto Pilot et al. [60]. Intense Raman signals are observed due to the Localized surface plasmon resonance (LSPR) of the NPs and the resultant lightning rod effect [61-63]. For RS variants like SERS, RRS, *etc.*, the incorporation of the metallic NPs makes it possible for their employment in theranostics, where photothermal therapy is used. Both Raman and SERS offer tremendous flexibility in instrumentation and can be portable for field applications [64, 65]. Portable SERS devices can enable fast point-of-care (POC) diagnostics [66, 67]. Moreover, when used in conjunction with genetic probes, SERS enables multiplex and ultrasensitive detection of nucleic acids produced from tumor, opening up numerous possibilities for early diagnosis and subtyping of clinical malignancy [68, 69].

Another variant of RS is RRS which has not yet been fully explored in the area of theranostics. In this technique, the incident radiation frequency should match with the electronic excitation of molecules, resulting in a 10^6-fold increase in the Raman signals [70, 71]. RRS assists in studying chromophores found in proteins, including chlorophyll carotenoids and iron clusters [72] [73]. Only a minority of the stretching vibrations of the analyte molecule are amplified under resonance conditions. RRS does not provide information about functional groups that are not involved in the electronic excitation of the molecule, as in the case of molecules having no chromophore groups [74, 75]. Hence, RRS is an alternative technique to study the vibrational modes of specific molecules containing chromophores [70] and can be tuned to reveal information about the 'biologically important' fraction of molecules.

In general, RS and its spectroscopic counterparts provide a better demonstration of numerous biomarkers associated with a particular disease, achieving a breakthrough in cell and tissue imaging [76]. The efficacy of RS was compared and analyzed by Harada and Takamatsu [77], Kendall *et al.* [78], and Almond *et al.* [79], respectively, for probing of dysplasia in Barrett's oesophagus. They discovered that RS had an 86 percent sensitivity and an 88 percent specificity in distinguishing high-grade dysplasia from adenocarcinoma *in vitro* [79]. Lakshmi *et al.* [80] have found a minor loss of lipids in ligamentous sites with no osteoradionecrosis and a complete loss of lipids in osteoradionecrosis bone for oral cancer patients treated with laser radiation therapy. Vidyasagar *et al.* [81] discovered spectral alteration in cervix cancer patients related to radiotherapy responses. Although minimal alterations in Raman spectra were noticed during radiotherapy, it was recognized that higher-resolution spectra could improve the analysis of results. Morris *et al.* [82] used Raman spectroscopic analysis to investigate the long-term effects of radiation on bone chemistry. Radiation-induced breakdown of collagen properties has been found in human cortical bone [83]. The Raman spectral features of radiation-induced bone mineral abnormalities were detectable after one week of irradiation that lasted for 26 weeks [80]. These unique diagnostic capabilities of RS, if combined with desirable therapeutic probes, can lead to the development of promising theranostic tools for the early diagnosis and treatment of various diseases.
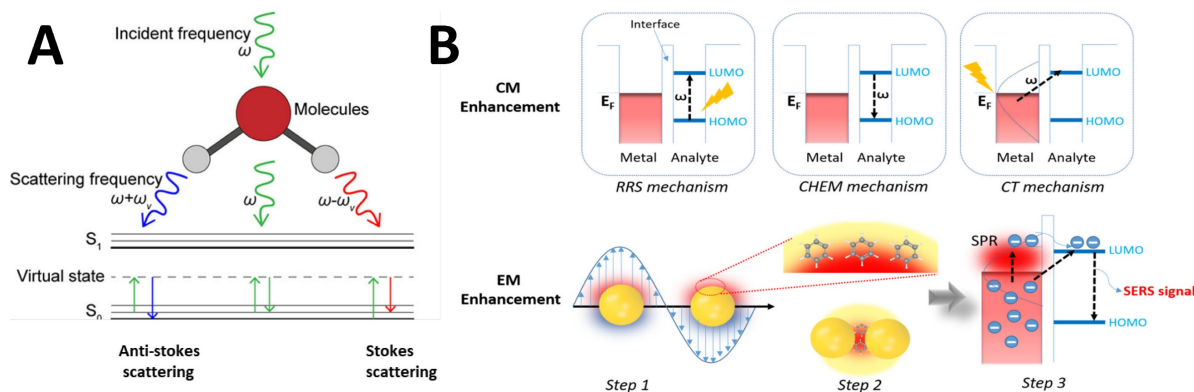
Figure 1: (A) Schematic representation of Raman scattering phenomenon. Figure reprinted from [47] with permission. Copyright (2021) Journal of Applied Physics. (B) Mechanism of enhanced SERS signal of analyte on the noble metal substrate due to electromagnetic and chemical field enhancements. Figure reprinted from [59] with permission. Copyright (2022) The Journal of Physical Chemistry C.
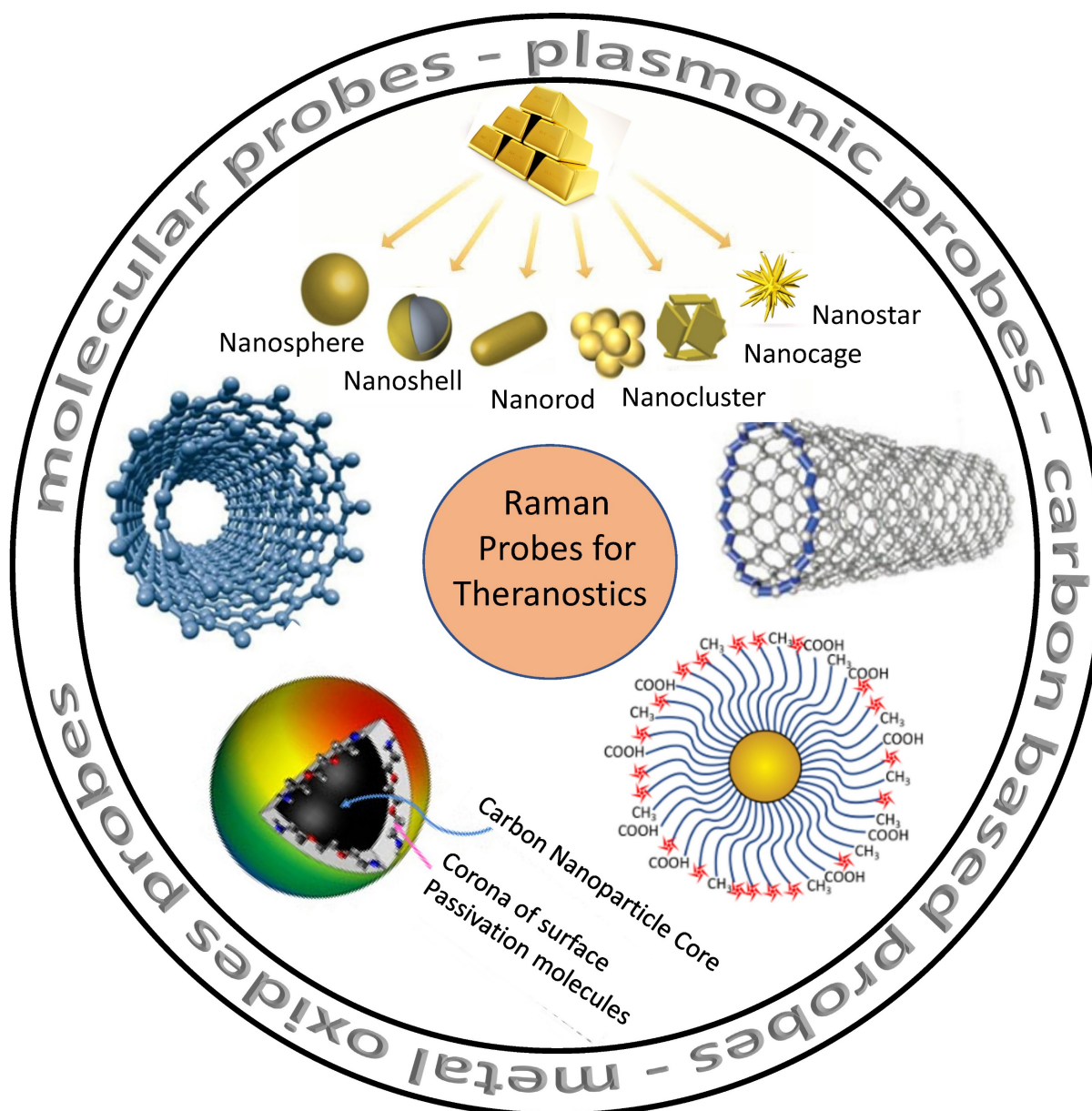
Figure 2: Various probes employed for Raman theranostics such as molecular, plasmonic, carbon, and metal oxide probes. Figure adapted from [84][85][86] with permission. Copyright (2019) Journal of Applied Physics, (2015) Frontiers in Chemistry, (2018) Jove-Journal of Visualized Experiments.

Raman Probes for Theranostics

Nanomaterials with RS could provide a brand-new optical detection and imaging technique. As seen in **Figure 2**, such nanomaterials serve as potential Raman probes [84-86]. Raman probes are tiny Raman-active moieties with high scattering cross-sections and can target, detect, and image biological entities, such as live cells, tissues, *etc.* [87]. Such probes can be of different types: molecular probes, plasmonic probes, carbon-based probes, metal oxides probes, and others, which can be used for concurrent therapy **(Figure 2)**. Using these functionalized probes for targeting specific biomarkers, Zavaleta *et al.* and Palonpon *et al.*

successfully demonstrated multimodal imaging in living subjects [88] [89]. Using a fiber-optic setup, Horgan *et al.* created a theranostic technique that allows *in vitro* real-time cancer diagnosis [90]. Such fiber optic setup will make it possible to side-step myriad faults in the current theranostic systems. Shamjith *et al.* [91] reported a quinoline-appended Iridium complex (QAIC) in the form of a molecular probe to be used in fluorescence and SERS modalities for the detection of nicotinamide adenine dinucleotide (NADH) that helps in the regulation of cellular metabolism. The detection limit of NADH was observed at 25.6 nM using luminescence and 15 pM for SERS. When exposed to endogenous NADH, QAIC showed a discernible, time-dependent

luminescence turn-ON response [91]. Joseph *et al.* have successfully eradicated cancer cells and cancer stem cells using targeted theranostic nanovehicle (TTNV). Raman fingerprint data was specifically used to study biochemical and structural changes in response to various treatments for TTNV [92]. The results suggested that the synthesized multipurpose nanocarrier substrate may improve PDT and Photosensitizer Fluorescence Detection (PFD) of gastric cancer tumors *in vitro*. In clinics, nanocarriers show much promise as theranostic agents for treating stomach cancer patients. Thus, Raman probes with tailored properties can lead to the simplification of existing theranostic tools. Some of these advanced Raman probes **(Figure 2)** that have the potential for theranostics are discussed in the sections below.

Molecular Probes

The development of theranostics depends on molecular probes, which are composed of small molecule moieties and nanosize probes like gold and silver NPs, carbon NPs, MagNPs, semiconducting nanoparticles, small organic molecules, etc. [93, 94]. These nanohybrid probes are widely used in theranostics because of easy surface modification, biocompatibility, imaging properties, and exceptional photothermal performance [95]. Such molecular probes also serve as efficient Raman reporters/tags. Transition metal-based molecular probes offer unique photophysical properties, long luminescent lifetimes, tunable metal toxicity, and better photostability [96]. Due to numerous advantages, these probes are versatile candidates for biomolecular probes [97, 98]. Late transition metals are incorporated in the probes, which accounts for the high decay lifespan and
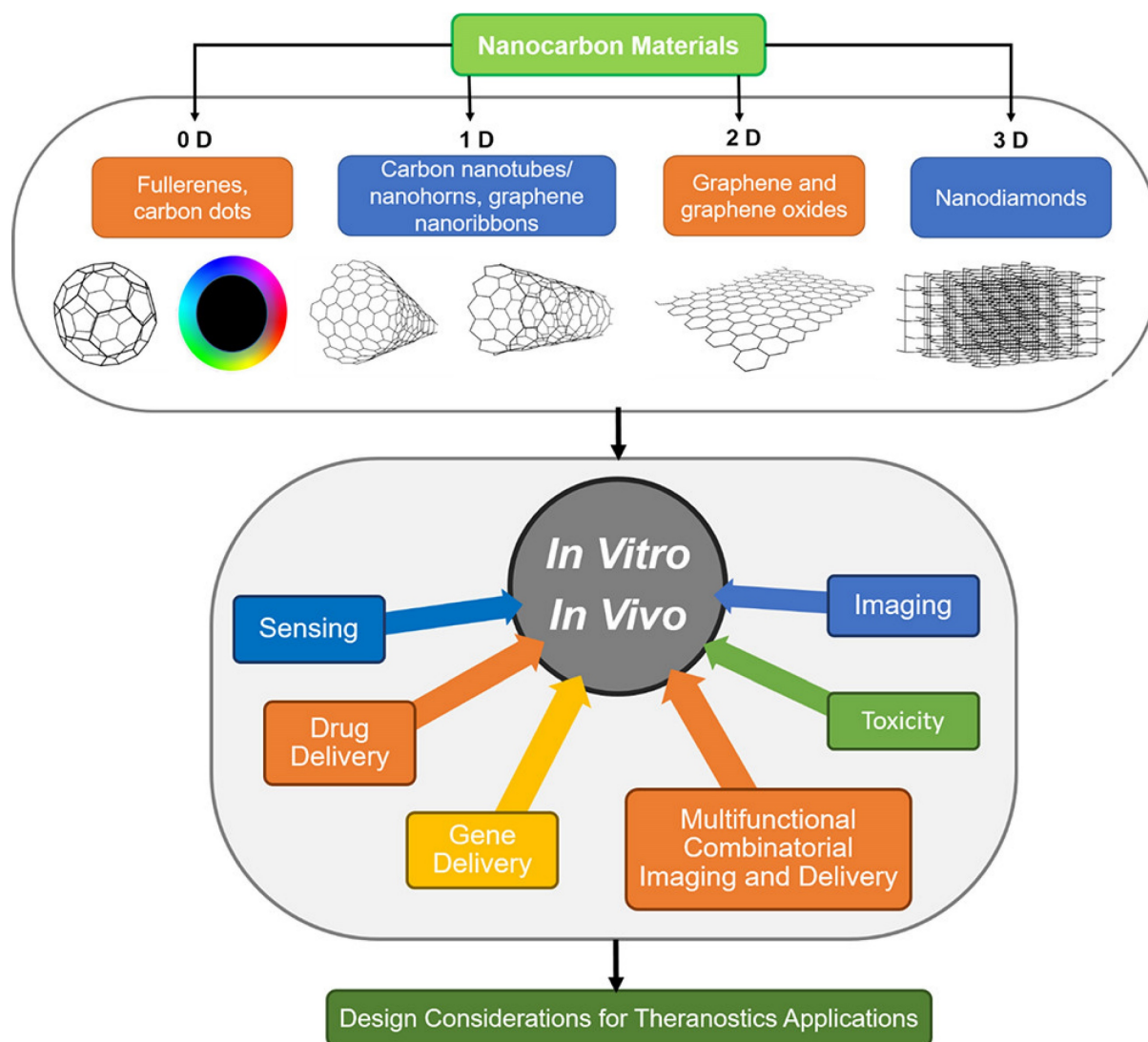
Figure 3: Various types of carbon-based probes with different dimensionality and utilization in theranostics applications. Figure reprinted from [105] with permission. Copyright (2019) Chemical Reviews.

reduces the autofluorescence background. Liu *et al.* used bipyridine Ruthenium (II) complex to monitor lysosomal formaldehyde in normal and tumor cells. This Ru (II) complex was reported as an effective tool for the detection of formaldehyde *in vitro* as well as *in vivo* [99]. In addition to Ru (II) complex, single molecular probes are used for high-contrast imaging and PTT. Using photoacoustic imaging, Meng *et al.* have created a Hypoxia-triggered single-molecule probe that enables centimeter-level deep tissue penetration and high-contrast visualisation of the tumor [100]. In another report, Meng *et al.* have also developed a dual-responsive molecular probe for tumor-targeted imaging and PDT [101]. The major benefits of these multifunctional molecular probes is their capacity for simultaneous diagnosis and real-time monitoring of biological processes. Molecular imaging probes can be utilized as non-invasive tools to aid in the early diagnosis of diseases and, more effective treatments [102].

Carbon-based Probes

Because of their excellent mechanical, electrical, thermal, optical, chemical, and peculiar structural dimensional characteristics, carbon-based nanomaterials have attracted a lot of attention in a variety of fields, including biological applications. They are potential candidates for tumor diagnostics due to their distinct Raman spectral features and ease of functionalization. In addition, the intrinsic two-photon fluorescence property in the near-infrared region can facilitate multimodal deep-tissue optical imaging in conjunction with RS [103]. According to their size, many carbon-based probe types can be divided into groups. Carbon nanotubes/nanohorns, graphene nanoribbons, fullerene, and carbon nanodots are 0-dimensional (0-D) materials, while graphene and graphene oxides are 2-D and nanodiamonds are 3-D. Several of these nanocarbon probes have been extensively used for biomolecules detection, drug delivery, and imaging of cells and tissues (**Figure 3**) [104] [105]. The needle-shaped carbon nanotubes (CNTs) with a high aspect ratio allow for more drug loading with minimal or no effects on cell penetration (**Figure 4A**) [33, 106, 107]. Robinson *et al.* have investigated the multimodal applications of single-walled carbon nanotubes (SWCNTs) for bioimaging and photothermal treatment of cancer (**Figure 4A**) [107, 108]. When coated with PEGylated phospholipids, these probes showed an optical absorbance and characteristic Raman spectra. Kim *et al.* developed a PEGylated CNT-based PEG-CNTs- ABT737 complex. It improved the treatment of lung tissues by specifically targeting mitochondria in malignant cells [109]. ABT737 is an inhibitory drug that can decrease the anti-apoptotic protein B-cell lymphoma-2 for the effective treatment of cancer (**Figure 4B**). The application of RS in rapid identification and targeted illumination of CNTs was shown by Bhirde *et al.* [110]. In this study, two types of carbon nanotubes (SWCNTs and multi-walled CNTs) were chosen and compared. These carbon nanostructures could transform light into heat because of the electronic transitions in van Hove singularities [111]. To promote prolonged dispersion and the best cellular absorption while preventing the harmful effect at lower concentrations, the CNTs were covered with a lipid-polymer coating. RS was used to monitor the CNTs within living ovarian cancerous cells (OVCAR8) using the G and G' bands appearing at 1500-1600 and 2600-2700 cm^{-1}, respectively. The significant Raman features of carbon-based probes are D, G, and 2D bands. The D band is due to the disordered structure of graphene corresponding to sp^2 hybridized carbon atoms. The G band appears at around 1580 cm^{-1} which is due to the E$_{2g}$ mode. It arises due to the stretching of the C-C bond. If there are some randomly distributed impurities or surface charges due to biomolecules, the G peak gets split into two peaks i.e., G peak (1583 cm^{-1}) and D' peak (1620 cm^{-1}). This is due to the coupling of vibrational modes of impurities with the extended phonon modes of graphene. Nergiz *et al.* investigated the effects of the carbonaceous and metallic nanostructures to create novel multimodal composite nano patches. These composites were made of graphene oxide (GO) layers doped with gold nanostars into the carbon polymeric network for PTT [112]. RS has also been employed in conjunction with transmission electron microscopy (TEM) and mass spectrometry to precisely monitor the transport of the graphene-based nano patches within human breast cancer cells, SK-BR-3. Such monitoring was achievable due to distinct Raman signatures of graphene that are defect (D) mode, graphitic (G) band, and the second-order defect mode at 1350, 1560-1590, and 2700 cm^{-1}, respectively (**Figure 4C**) [113]. The spectral data obtained from the GO-Au nanostar composites revealed peaks with three times increased intensity for the D and G bands compared to pure GO. Song *et al.* designed CNT in an integrated ring (CNTR) configuration through a polymerization redox mechanism and partial doping of AuNP [114]. The nanocomposite could be used as a Raman sensor to locate cancerous cells in conjunction with a PA contrast agent to detect a tumor spot (**Figure 4D**) [114]. Due to the strong electromagnetic field hotspot, the SERS spectral intensity of CNTR doped with AuNPs was 110 times more enhanced than CNTR. The incorporation of CNTR with the glioblastoma cells in the brain showed that the nanostructure was

efficiently absorbed, with overall signal strength increasing with the number of cells. Beqa *et al.* introduced a remarkable nanocomposite by attaching gold nano-popcorn with SWCNTs for targeted diagnosis and PTT of cancer cells [115]. PTT was carried out for 10 minutes with a 785 nm laser, which caused a temperature rise of 60°C, killing over 95 percent of the cancer cells. Additionally, intense Raman signals due to D and G bands of SWCNTs hybrids were observed in the tumor-specific areas. This hybrid nanotechnology-based assay was quick since it only took 20 minutes for a cancer cell to connect to the probe and be detected and eliminated. [115]. Another type of carbon-based probes, the cucurbiturils (CB[n]s), are gaining popularity due to their unique supramolecular properties, which also make them ideal for precisely managing hot spots of the plasmonic NPs [116]. Additionally, Raman-sensitive CB[n]s can selectively trap analytes into the "hotspots" through a variety of interactions, including donor-acceptor, hydrogen bonding, and

other interactions that allow for precise molecular recognition. As a result, microfluidics has been used to create SERS substrates that contain CB[n]s functionalized noble metal NPs (NMNPs). Due to the distinct host-guest features of Raman-active substrates, guests might be selectively restricted inside the "hotspot" nanogaps (voids of CB[n]s) for efficient sensing and diagnosis [117]. Self-assembled NP probes are also gaining appeal as theranostic agents that are Raman active and paved the way for high-resolution *in vivo* imaging. These probes only form specifically inside cancer cells. Recently, it has been shown that Olsalazine can self-assemble *in vivo* into NPs when conjugated with a benzothiazole compound and a cell-penetrating peptide. When it is cleaved by furin, it gets overexpressed in specific cancers [28, 118]. In conjunction with NP and carbon-based probes, RS and confocal imaging can identify tumor margins precisely using high-resolution image-based surgery.
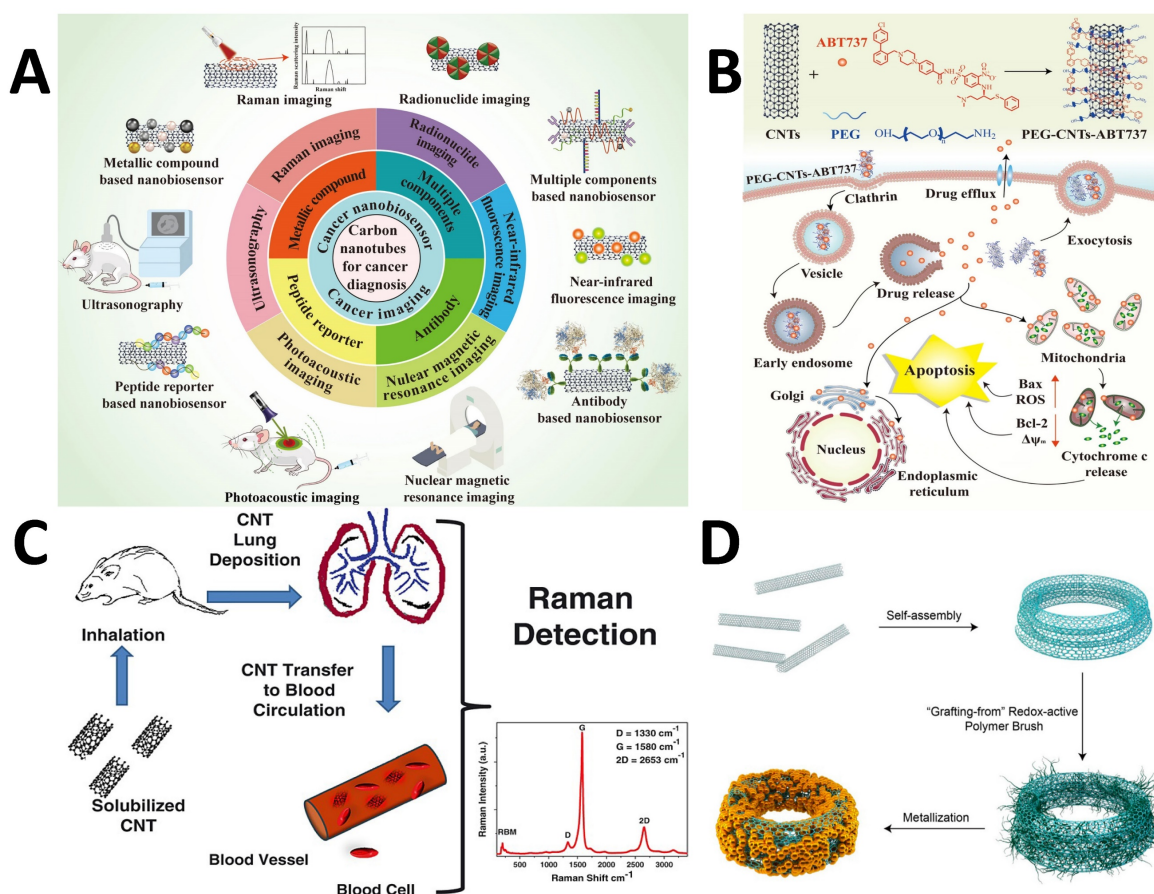
Figure 4: (A) Different applications of CNT for cancer diagnosis. Figure reprinted from [107] with permission. Copyright (2021) Journal of Nanobiotechnology (B) Working mechanism of PEG-CNT-ABT737 for treatment of lung cancer cells. Figure reprinted from [107] with permission. Copyright (2021) Journal of Nanobiotechnology. (C) Mechanism of transfer of CNT to blood circulation for treatment. Figure reprinted from [113] with permission. Copyright (2013) Journal of Applied Toxicology. (D) Self-assembly of CNTs into a CNT ring (CNTR) via redox-active poly(4-vinylphenol) (PvPH) brushes. This utilizes a surface-initiated atom transfer radical-polymerization (SI-ATRP) technique to convert Au³⁺ to Au (0) and encapsulate the CNTR with AuNPs. Figure reprinted from [114] with permission. Copyright (2016) Journal of American Chemical Society.
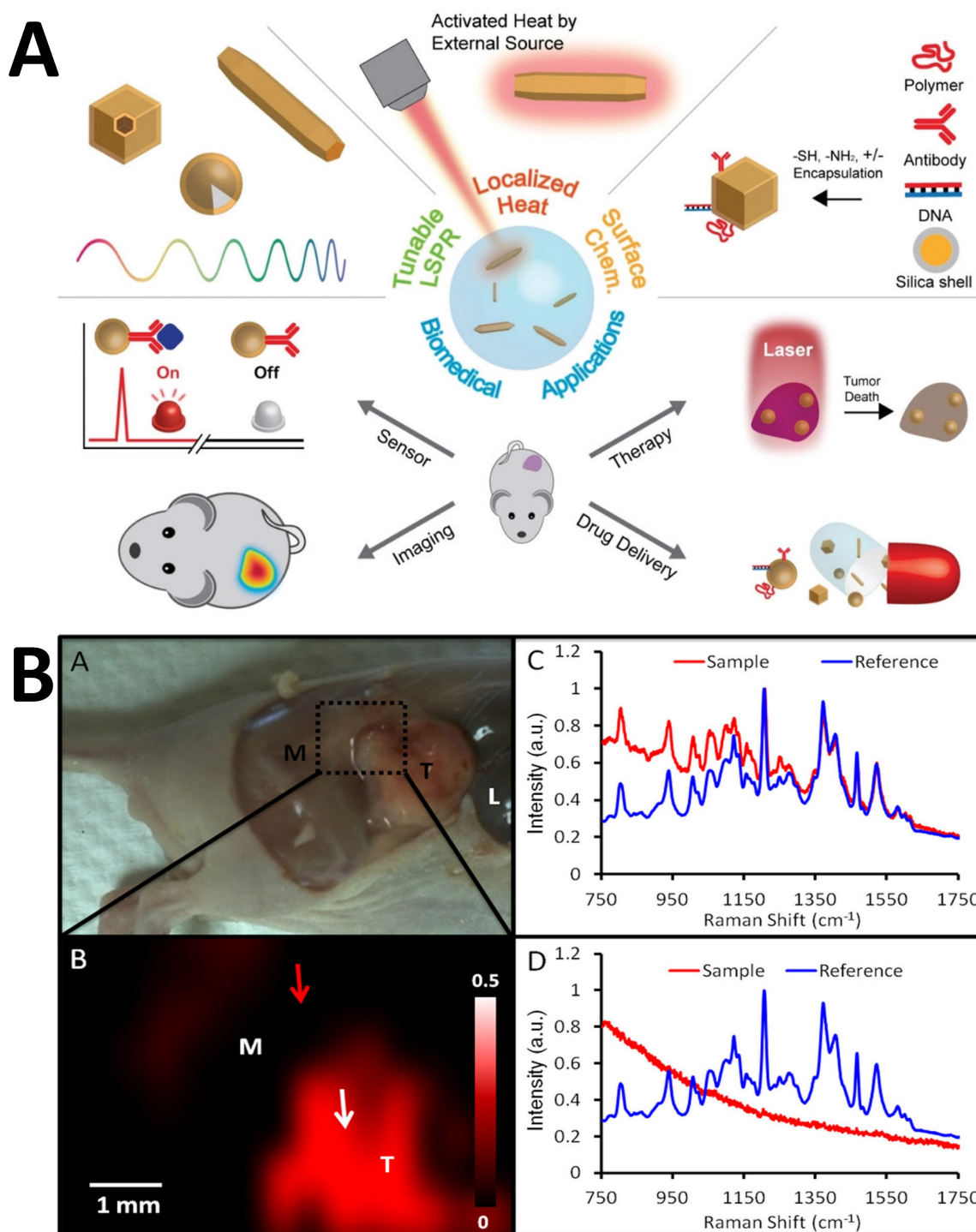
Figure 5: (A) Applications of plasmonic NPs in biomedical applications. Figure reprinted from [123] with permission. Copyright (2019) Advanced Science. (B) SERS imaging for identification of tumor margin. The red part imaging area shows the increment in the tumor. Figure reprinted from [125] with permission. Copyright (2012) ACS Nano.

Plasmonic Probes

Noble metals and their nanohybrids, such as core-shell structures, polymeric composites, NPs embedded in 2D materials, etc., are included in the category of plasmonic NPs that are referred to as plasmonic probes. Organic or dye molecules can be attached to the surface of plasmonic nanoparticles that act as SERS tags. Using multiple SERS tags in a probe can lead to efficient multiplexed detection of biological species with low detection limits, high sensitivity, selectivity, and photostability [119, 120]. Molecules can be combined with SERS tags to form an immunocomplex whose structure disintegrates and releases Raman probes, causing signal alterations [121]. Similarly, SERS-based aptasensors have

significantly progressed in the area of food safety [122]. To monitor medicine distribution and support PTT and PDT, the NP-Raman combination (manifested through SERS) may be combined with various theranostic techniques (**Figure 5A**) [123].

Zavaleta *et al.* suggested a strategy where they developed Raman endoscopy as an alternative to colonoscopy or conventional endoscopy [124]. The researchers proposed a new, flexible, fiber-optic-based Raman spectrometer connected to a single-mode fiber laser that can be added to the endoscopic device to create a multiplexed molecular imaging endoscope. Such a setup does not require any contact and remains free from contamination. A contrast agent made of Au was designed and further divided into batches, each of which was functionalized with ten distinct Raman active compounds. Jokerst *et al.* proposed the potential of coupled PA-SERS to bypass the comparatively modest Raman penetration limit [125]. Au nanorods were utilized as the imaging probes that harnessed the enhanced permeability and retention effect for *in situ* identification of ovarian cancers in mice and for determining the subcutaneous margins of tumors (**Figure 5B**) [125]. The researchers also proposed that with some specific aspect ratio and Raman active analyte, a massive enhancement in the PA signal was observed, which could persist for more than two days [125]. By examining microcalcifications type II with Au@SiO$_2$ nanoparticles, Liang and Zhang *et al.* found that SERS, unlike Raman, could easily distinguish benign breast cancer and *ex vivo* premalignant lesions in biopsied breast tissues, normal breast tissues (NB), atypical ductal hyperplasia (ADH), fibroadenoma (FD), invasive ductal carcinoma (IDC), and ductal carcinoma *in situ* (DCIS) [126, 127]. Colloidal AgNPs were used by Mert *et al.* to distinguish between malignant and normal cells in biopsied samples taken from the kidneys of healthy individuals as well as those with transitional cell carcinoma (TCC) and renal cell carcinoma, two kinds of kidney cancer (RCC) [128]. Feng *et al.* reported that the implantation of AgNPs in nasopharyngeal cancer helps differentiate between two types of carcinomas (C666 and CNE1) from the normal cell lines (NP69) [129]. The blood plasma of 34 healthy participants and 32 gastrointestinal cancer patients were detected and spectrally characterized [130]. In a separate study, Feng *et al.* demonstrated that the band assignments of SERS spectra revealed some changes in the cancer-specific tissues, comprising exceptionally elevated quantities of nucleic acid, phenylalanine, collagen, phospholipids, a lower proportion of amino acids, and saccharides in the blood plasma of a patient suffering from gastric cancer [131, 132]. In comparison to the healthy group, the SERS spectral bands around 725 and 1445 cm^{-1} are elevated for the group with gastric cancer. Ito *et al.* adapted a hexagonal-shaped nanostructure of silver mounted on the surface of a phosphor bronze fabricated chip used during serum investigation of colorectal and gastric cancer [133]. They studied the identification of positively-charged blood components such as tumor-associated antigens (TAA), tumor-specific antigens (TSA), and immuno-globulins (Ig) using the negatively charged surface of AgNPs. The blood peak height in SERS spectra was higher in the cancer patient's tissue and continued to rise as the malignancy progressed [133].

SERS has been used to screen urine samples for prostate cancer [134]. Kneipp *et al.* coupled AuNPs with living cells to get deeper insights into the structure of phenylalanine and DNA in cells [135]. Cottat *et al.* utilized Electron-Beam Lithography (EBL) to construct a newly developed SERS technology based on a nano-antenna biosensor made of Au to identify biomarkers in the nano-molar range of concentrations in distinct bio-fluids (serum and saliva) as well as the manganese superoxide dismutase generated by cancer infected liver [136].
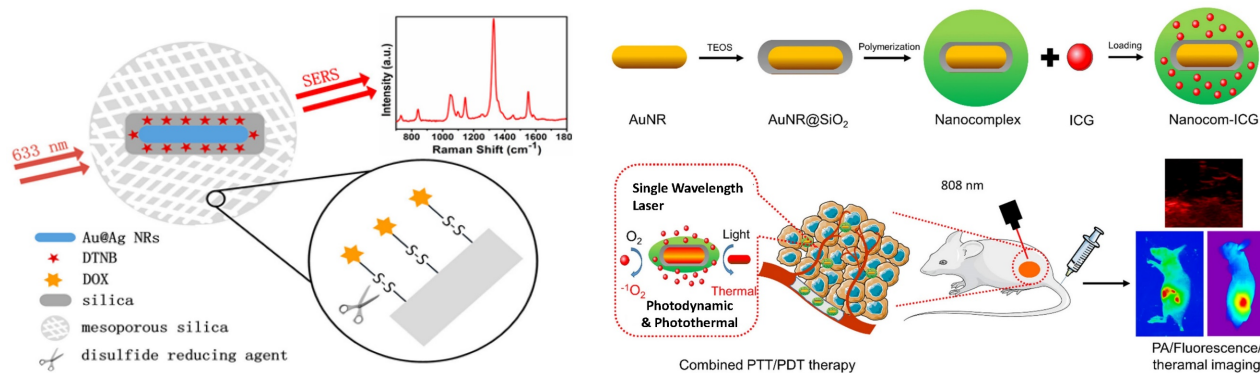
Figure 6: (A) Scheme where disulfide bond acting as a nanocarrier in intracellular drug delivery scheme. Figure reprinted from [138] with permission. Copyright (2013) Analytical Chemistry. (B) Fabrication of Nanocom-ICG in combination for PTT/PDT therapy. Figure reprinted from [142] with permission. Copyright (2021) Journal of Nanobiotechnology.

Madathil *et al.* have fabricated a novel SERS-based catheter device using 30 nm size AgNPs decorated over leaf-like TiO_2 nanostructures. This device can differentiate between normal, premalignant, and malignant tissues and allows rapid detection, classification, and grading with high accuracy and sensitivity [137]. Zong *et al.* employed the SERS technique to understand the mechanism behind the doxorubicin (DOX) released inside the cells by tracking down the pathway of the nanodrug [138]. The DOX was covalently linked to the mesoporous silica (MS) through a disulfide linkage, utilizing the principle of tracing Raman/fluorescence signals to identify intracellular drug delivery. The researchers used Au@Ag nanorods labeled with 5,5′ dithiobis-(2-nitrobenzoic acid) (DTNB) and MS to demonstrate the involvement of glutathione (GSH) in DOX release **(Figure 6A)** [138]. Lui Z. *et al.* [139] proved the use of Raman for diagnosing tumors through bio-imaging and theranostic applications at the same time without using dye [139]. Qian *et al.* [140] reported a scheme in which PEGylated AuNPs were conjugated to tumor-targeting ligand like single-chain variable fragment (ScFv) antibody and systematically injected into mice. Due to their emission in near-infrared windows, they were able to target tumor biomarkers. The difference in SERS intensity by tumor was observed for targeted and non-targeted NPs. This finding demonstrates that EGFR-positive tumors were successfully targeted *in vivo* by the ScFv-conjugated AuNPs [140]. Zhang *et al.* constructed a multipurpose plasmonic theranostic substrate for SERS imaging and drug-photothermal treatment using a mesoporous titania-based yolk-shell nano-particle [141]. The idea was to build a single NP that combined the conventional chemotherapy, PTT, and one enhancing reagent for better SERS imaging. Gong *et al.* created a nanoprobe made of thermally sensitive polymer enclosed by AuNRs integrating with incorporating Indocyanine Green (ICG) for tumor treatment [142]. The thermal-sensitive polymer coating significantly enhanced drug uptake capacity and also increased ICG stability by boosting ICG J-aggregate generation and promoting targeted ICG deposition in the tumor location. This study suggested that nanocom-improved ICG's therapeutic performance was due to coordinated PTT/PDT therapy following NIR laser irradiation **(Figure 6B)** [142]. Several reports by Gambhir and Kircher have demonstrated the use of SERS in multimodal imaging of various pathologies [124, 125, 143, 144]. A unique triple-modality MPR nanoparticle has been reported, which stands for magnetic resonance imaging, photoacoustic imaging, and Raman imaging (MPR) that has the potential to delineate the margins of tumor cells up to picomolar sensitivity both *in vivo* as well as *in vitro* using mice as a model. MPR has provided a way to monitor a surgery preoperative as well as in an intraoperative manner. This aids in the tumor diagnosis in a more detailed and extensive manner with better precision [144]. SERS has also been used to improve the detection and resection of nonmuscle invasive bladder cancer [145]. Interestingly, it was found that passively targeted nanoparticles had a better rate of penetration and concentration in the cancerous human bladder tissues due to enhanced permeability and retention. SERS could clearly delineate between healthy and diseased tissue when antibody-based, and tissue permeability-based targeting mechanisms were used [145]. Additionally, transurethral resection (TUR) was guided by multiplexed Raman cystoscopy, and it could detect residual disease, which is generally not observable by traditional white-light cystoscopy [145]. A miniature, non-contact opto-electro-mechanical Raman device similar to optical endoscopes has been designed to obtain multiplexed molecular SERS data from patients [143]. Photoacoustic imaging can also be used in conjunction with SERS, as demonstrated by Gambhir *et al*. [125], where subcutaneous xenografts of the ovarian cancer cell lines in living mice were imaged with PA imaging and the tumor margin separating cancer and diseased tissue sections could be efficiently delineated by SERS. Core-shell NPs with multimodal capabilities also play a crucial role in diagnostics and therapies. The core-shell NPs of methylene blue-loaded gold nanorod@SiO_2 (MB-GNR @SiO_2) were synthesized for medical diagnostics and dual PDT [146]. Similarly, Feng *et al.* investigated the bioconjugation of Au nanobipyramids (Au NBPs) with Raman reporter 2-naphthalenethiol (2-NAP) and folic acid to specifically kill and detect MCF-7 breast cancer cells based on photothermal and SERS properties of Au NBPs. This plasmonic substrate allows ultrasensitive *in vitro* detection and *in vivo* SERS imaging of MCF-7 cancer cells [147]. Among variable potential plasmonic substrates, gold nanostars (AuNSs), due to their multiple sharp branches, have emerged as 'one for all' plasmonic substrates for cancer theranostics, PA, and photo-thermal conversion effect [148, 149]. Similarly, plasmonic substrate multilayered GNRs are very stable in solutions like NaCl, phosphate-buffered saline (PBS), and culture medium. The stability provides a way to use them for biological purposes, as most biological reactions are in the pH range of 4-8. Contrarily, various imaging methods based on GNRs have been successfully developed, including dark-field scattering imaging, PA, and two-photon luminescence, all of which have quick or even

real-time responsiveness in theranostics [150]. While the clinically translatable nanoparticle probes typically used in MRI imaging have been studied extensively for their toxicity and biodistribution profiles, such studies are also being conducted for *in vivo* SERS, and their enhanced accumulation in diseased tissues results in obtaining enhanced biochemical signatures for diagnostic and therapeutic purposes [151, 152].

Metal Oxide Probes

Metal oxides are the most intensively explored semiconducting materials, such as Fe_3O_4, Fe_2O_3, $MnFe_2O_4$, and $CoFe_2O_4$, for multiplexed applications in MRI, drug delivery, *etc.* [153]. In this regard, Yamada *et al.* [154] have investigated the crystals of TiO_2 (001) and NiO (110) using SERS [155]. They described that the charge transfer of the adsorbate–adsorbent interactions resulted in an amplification of Raman scattering due to the chemical interaction in the molecular sites of NiO or TiO_2 and nitrogen of pyridine. Nb_2O_5 NPs were discovered to be a new semiconducting SERS substrate that can replace noble metals and has a number of applications in biology [156]. The chemisorption of dye on Nb_2O_5 resulted in forming new bonding and antibonding molecular orbitals that can facilitate charge transfer more efficiently with longer excitation wavelengths. Other NPs, such as tungsten oxide, also have interesting properties which can be harnessed for drug delivery, PDT, and PTT [142]. *In vitro* and *in vivo* studies have already been conducted using substoichiometric tungsten oxide (WOx) nanostructures coated with biocompatible substances [157]. Lin *et al.* [158] have optimized Fe_3O_4 nanoparticles that possess excellent SERS activity and can probe up to $5*10^{-9}$ M concentration of crystal violet. They have optimized the design of the Fe_3O_4-based bioprobe in such a way that they can perform dual-mode cancer imaging using SERS and MRI [158]. With a Fe_3O_4-based bioprobe, subtypes of cancer cells were successfully identified with high sensitivity and specificity *in vitro* via high-resolution SERS imaging. The capability to probe a tumor at an early stage using a unique bioprobe with dual-modal imaging capability is crucial for detecting and treating cancers [158]. Metal oxides can be used for oncological imaging *in vitro* because they have the potential to show excellent SERS activity, which can be utilized to differentiate between cancerous and normal cells. They can also be used as a high-potential contrast agent for T1-weighted MRI, enabling active-targeted imaging of tumor tissues *in vivo* [158]. Among various metal oxides, the NPs of iron oxide are the first generation of nanomaterials approved by the food and drug administration for their use in bioimaging, i.e., MRI, for the treatment of iron deficiency [159]. NIR-responsive multifunctional MagNPs with remote-control photothermal ablation have been designed by Abedin *et al.* [160] for the photothermal treatment of breast cancer. These $Au-Fe_2O_3$ NPs were designed for medical imaging and treatment of breast cancer cells. Au was used as a coating material because it could enhance the photothermal effect by introducing surface plasmons in the NIR region [160]. The combined effect of surface plasmon resonance and superparamagnetic properties of Fe_2O_3 provides a multimodal platform for nano thermal ablation and MRI. Rissi *et al.* [161] observed an interesting effect of doping zinc oxide NPs with aluminum, gallium, and indium on optoelectrical properties. The doping results in enhanced absorption in the near IR region and emission range in green-yellow, orange-red, and blue-violet, depending upon the doping element. At concentrations below 60 g/mL, ZnO NPs doped with Al^{3+}, Ga^{3+}, and In^{3+} were harmless to tumor cells. Only high doses (60–100 g/mL) of doped NPs revealed considerable toxicity after 24 hours of incubation. The potential of ZnO NPs for cell death in human tumors and healthy cell lines were also investigated *in vitro* [161]. Interestingly, ZnO NPs can stop the early leakage of medications under physiological circumstances [162]. It can serve as a therapeutic agent since Zn^{2+} produced by the decomposition of NPs can also overcome the tumor's resistance to 5-fluorouracil (5-FU) and control a number of physiological processes that restrict tumor growth [162]. The fluorescence of these nanoprobes can also be enhanced by forming plasmonic conjugates, and concurrently, these plasmonic conjugates can enable SERS detection and imaging in addition to the therapeutic effects of the nanoprobes [162]. One such example is a study by Han *et al.* [163], where a multifunctional Fe_3O_4/Au cluster/shell nanocomposite for the SERS-assisted theranostic method was fabricated. The use of Au with metal oxide was reported for the first time for prostate-specific antigen detection, MRI, and magnetic hyperthermia. Moreover, these Fe_3O_4/Au nanoparticles demonstrated superparamagnetic properties, strong r2 relaxivity, uniform magnetic heating action, and low toxicity, providing a non-contact method with fewer side effects compared to an existing traditional theranostic method like chemotherapy or radiotherapy [163]. At the same time, the SERS enhancement could unambiguously detect prostate cancer. While MRI can pinpoint a tumor's site, SERS is a good option for diagnosing prostate cancer and elucidating its tumor margin due to its higher resolution [163]. A variety of SERS nanoprobes, including plasmonic NPs, Au

NBPs, CNTs, and plasmonic magnetic NPs, together with their corresponding TEM images and SERS spectra for the specific detection of malignant cells and tissues are shown in **Figure 7**. In the current generation of cancer medications, achieving real-time therapy response monitoring is of the utmost importance. Therefore, we can infer that incorporating plasmonic materials with metal oxide NPs provides a way for better theranostic intervention in real-time. Such a combination makes them simultaneously suitable for multiple applications such as MRI, magnetic hyperthermia, and SERS.

Other Probes

There are various probes from the families of MagNPs, quantum dots (QDs), and activity-based probes that can be utilized as theranostic agents in addition to plasmonic, metal oxide, and carbon ones. The use of MagNPs to carry drugs has recently attracted a lot of attention as a viable tool for cancer treatment [164]. The core or the shell of NPs can also be magnetic, rendering unique capabilities to these nanoprobes. MagNPs combined with gold or carbon nanomaterials possess enhanced optical properties that can be used for MRI [165]. Jibin *et al.* have fabricated a plasmonic magnetic nanoprobe of iron-oxide hybrid nanoparticles decorated with graphene and gold for SERS imaging, self-guided magnetic resonance, chemodynamic therapy (CDT), and PTT [166]. This delivery technique has fewer adverse effects than conventional chemotherapeutic medicines and can administer therapeutic agents to specific locations. The therapeutic agents (e.g., doxorubicin, idarubicin, paclitaxel) can be bioconjugated with a polymer coating of MagNPs, followed by their delivery inside the body [167]. Cancer-specific antibodies or folic acid can also be added to these multifunctional MagNPs. Following regulatory approval, clinicians can use newly designed devices that combine multifunctional MagNPs to take better therapeutic action for cancer patients [165]. Similarly, zinc QDs have been used in the diagnosis of cancer cells. The *in vivo* studies by Xiao *et al.* [162] of these zinc QDs have shown excellent ability to deliver doxorubicin and 5-FU in the tumor microenvironment. As a result, both conventional and sophisticated Raman probes can be employed as effective theranostic probes for the early diagnosis and treatment of disease.
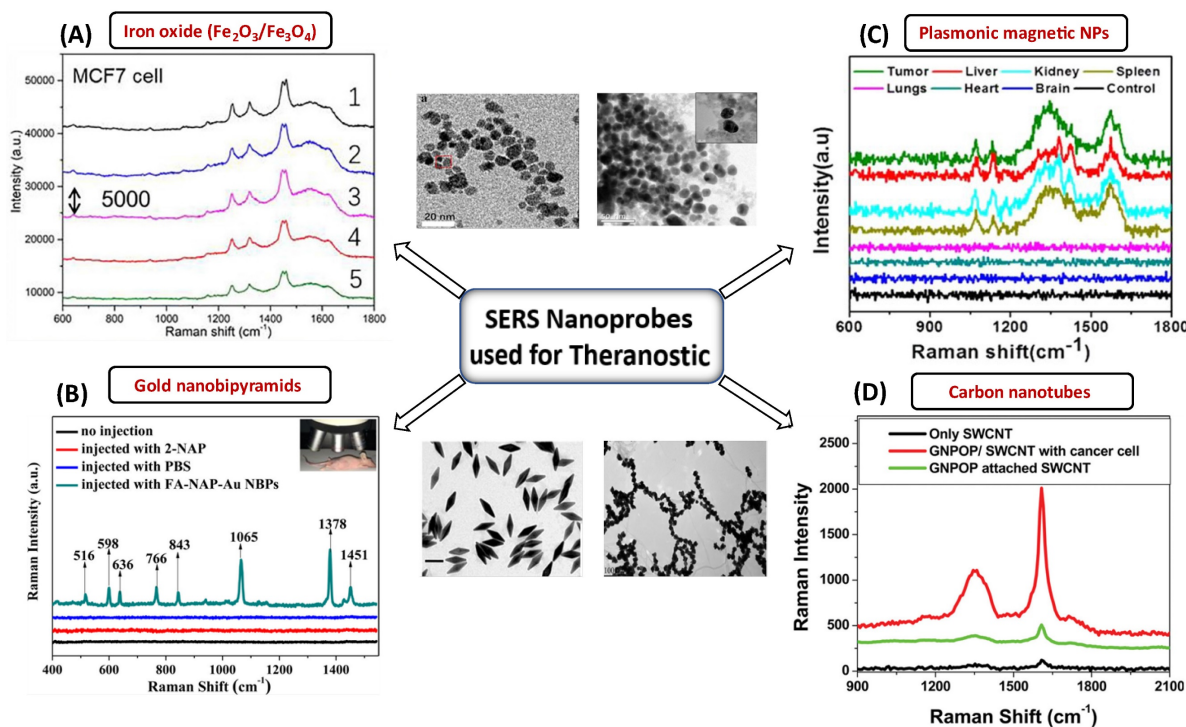
Figure 7. SERS nanomaterials used for the diagnostic purposes (A) Iron-oxide NPs to differentiate between cancerous and normal cells collected from 5 different spots laser in rabbit blood samples. The significant Raman signature bands are at around 1255 cm^{-1} (C=O stretching) and 1325 cm^{-1} (CC stretching) observed for targeted tumor cells. Figure reprinted from [158] with permission. Copyright (2022) Fundamental Research. (B) The detection of MCF-7 cancer cells based on SERS properties of conjugated Au NBPs. The prominent bands are observed due to binding of these AuNBPs with MCF-7 cancer cells. Figure reprinted from [147] with permission. Copyright (2017) ACS Biomaterials Science & Engineering. (C) Plasmonic magnetic NPs for intensity profiling of various organs in tumor areas. The spectral intensities at 1330 and 1090 cm^{-1} are enhanced for tumor targeted areas. Figure reprinted from [166] with permission. Copyright (2021) ACS Applied Bio Materials. D) SERS based cancer cell detection using gold nano-popcorn with SWCNTs. Significant Raman bands at 1300 and 1590 cm^{-1} that correspond to the (D and G) band of SWCNTs were observed for malignant tissues. Figure reprinted from [115] with permission. Copyright (2011) ACS Applied Materials & Interfaces.

Activity-based probes (ABPs)

ABPs are a different class of tiny molecules that frequently bind to the target enzyme's active form via covalent binding. The biological target is inhibited and labeled by these ABPs, which have the ability to target a wide range of proteases [168]. Cathepsins and proteases, for instance, are used in theranostic procedures. The increased levels and activity of cathepsins in a variety of human cancers make them useful markers for early detection and the identification of therapeutic targets. Yael *et al.* developed small molecule-based quenched activity-based probes that allow both the detection and simultaneous treatment of cancer cells [169]. In conclusion, theranostic probes for SERS and Raman can be widely used to deliver and detect therapeutic substances (including ablation and photothermal therapies). Such a system is ideal for theranostics because the nanoprobes have the properties needed to deliver therapeutic agents, selectively and quickly accumulate in diseased tissue, report the biochemical and morphological characteristics of the region, deliver therapeutic agents, biodegrade, and be safe for healthy tissues. The possible clinical applications include therapy, drug delivery, image-guided tumor margin delineation, labeled or label-free identification of malignant tissues, and finally, non-invasive and label-free assessment of the metastatic potential of the tumors [170].

The overall view of the Raman probes, including their pros and cons in various theranostic tools, has been summarized in **Table 1**.

Mitigating the challenges of the use of Raman and SERS in theranostics

Through the development of suitable instrumentation, it has been possible to incorporate RS in non-invasive and *in vivo* probing of living systems as well. However, many optics-based methods are limited by low light penetration into tissues compared to other imaging techniques, such as MRI, and RS is no exception [171-173]. Thus, this technique is most suitable for lesions or neoplasms on the surface or can be accessed endoscopically or intraoperatively. Therefore, Raman's limitation to only probe surfaces despite the proven safety and efficacy of the tool requires further research and development of probes and instrumentation. Advanced Raman instrumentation, such as confocal Raman microscopy, SORS, etc., has aided in imaging with better penetration depths and improved spatial resolution [173]. The integration of RS with novel substrates, such as MPR NPs, NIR-active quantum dots, etc., has also enhanced the penetration depths in deep tissue imaging.

Table 1. A brief summary of Raman probes with their pros and cons in theranostics

SI.No.	Nanoprobes	Constituents	Techniques used	Pros and Cons	References
1	Carbon based probes	Carbon nanotubes Graphene oxides Fullerene Nanodiamonds	Raman/SERS PTT	PROS: Ease of functionalization, variable morphological transition, biocompatible, economical, PDT CONS: Non-biodegradable, cytotoxicity	[104, 105, 107, 108, 110, 111, 112, 114, 115, 117, 118, 120]
2	Plasmonic probes	Silver and gold nanoparticles Gold nanorods Core-shell plasmonic NPs	Raman/SERS PA PDT PTT Multimodal imaging	PROS: Inertness, plasmonic properties, easily tunable, biocompatible, ease of functionalization, antimicrobial effects, high molecular specificity, selectivity and photostability, multimodal imaging CONS: Localized heating may cause damage to tissues, cytotoxicity, costly	[44, 122, 123, 128, 129, 130, 131, 132, 137, 139, 140, 142, 147, 148]
3	Metal oxides probes	Fe_2O_3 Fe_3O_4 TiO_2 NiO ZnO Nb_2O_5	Raman/SERS PDT PTT MRI	PROS: Antibacterial activity, large durability and stability, inherent imaging characteristics, phytogenic properties CONS: Cytotoxicity, low stability, generation of reactive oxygen species	[153, 155, 156, 158, 159, 160, 161, 162]
4	Transition metal-based probes	Ruthenium Platinum Iron complexes	Fluorescence Luminescence PDT	PROS: Unique photophysical properties, bioimaging, stability, luminescence CONS: Cytotoxicity, heavy metals accumulation in the body	[99, 100, 101, 102, 161]
5	Other probes	Magnetic NPs Quantum dots	Raman/SERS PTT CDT	PROS: High resolution imaging, good contrast agent in MRI, biocompatibility CONS: Prone to aggregation, high cost, poor sensitivity, toxicity, limited by the external magnetic field	[35, 163, 164]

RS has an inherently low scattering cross section, much lower than fluorescence [174, 175]. The autofluorescence background often makes it challenging to get a discernible spectrum and complicates the Raman spectral analysis under *in vivo* conditions, specifically under slow imaging [176]. However, these problems can be overcome by using a near-IR laser which ensures a much lower fluorescence background, and also by using a fast scanning spectrometer which can either do point, line, or raster scanning using a rotating galvo-mirror [177]. The use of near-IR lasers also ensures higher tissue penetration depth and minimum absorbance by the biological medium. The laser can also be guided to the appropriate areas of analysis through special light collection probes in the form of needles or endoscopic setups. The problem of scattering cross-section can be resolved through advanced RS techniques where even single-molecule detection is possible, thus bringing it at par with the sensitivity of fluorescence methods [178]. These interventions help overcome the limitations of using RS or SERS for *in vivo* applications [179].

The low photon count resulting from low scattering cross-section in RS results in significant noise in the spectrum, particularly in biological systems where low laser power is required to avoid the burning of the samples [177]. The background fluctuations generated by the instability of the laser excitation source, background fluorescence signals, or pixel-to-pixel variations in the detector are significant sources of noise and diminish the reproducibility of signals even at large acquisition times [180]. Another form of noise is the dark current, a random stream of electrons thermally activated in the semiconductor-based detector [181]. These noises can be reduced by optimizing the Raman system's components, specifically the detector's quantum efficiency, and further sampling the signals by an analog-digital converter [182]. Decreasing the detector's temperature also helps reduce the thermal noise to a great extent [183]. Several data processing techniques, along with software-based denoising techniques which use advanced chemometric methods and machine learning algorithms, can reduce these noises to a great extent [184]. Denoising algorithms and spectral smoothening techniques, such as the Savitzky-Golay method, are now routinely integrated with spectral acquisition software [185-188]. The use of a reflective substrate for the samples has also been shown to enhance the signal-to-noise ratio (SNR) [189]. Additionally, water immersion objectives are often used to prevent damage to biological samples [177]. Techniques such as shifted excitation Raman difference spectroscopy (SERDS) can also be used to remove the fluorescence background in RS and have been demonstrated to be effective in *in vivo* imaging of biological samples [190-193].

The data analysis of the sample involving Raman and SERS is not straightforward, particularly in the label-free modality for biological samples. Biochemical species such as proteins, lipids, nucleic acids, carbohydrates, etc. make up biological systems, and the spectra of a cell, tissue, and bacterium may look remarkably similar to inexperienced eyes [177]. This makes the application of RS challenging due to lack of specificity and significant spectral overlap of the various biological constitutents. Several chemometric techniques that heavily rely on supervised or unsupervised machine learning algorithms can effectively observe this minor spectra fluctuation. The use of RS in biology has profited from the recent boom in machine learning techniques [194]. The usage of Raman tags using Raman reporter often has some intrinsic disadvantages which affect their biocompatibility, involve high cost, offer limited variety, and are often difficult to tag [149]. The stability of the tags in physiological conditions is also an issue and might affect the reliability of the data analysis [119, 120]. Therefore, for both Raman and SERS, there is an option to employ the label-free modality, which does not involve the use of any exogenous fluorophores. While the nanoparticle itself may be useful for therapy using photothermal effect etc., the plasmonic coating can enable direct SERS data collection from cells and tissues [195, 196]. Additionally, SERS commonly suffers from reproducibility of the signals due to the difficulties in controlling the nanoparticle assemblies and the intense electromagnetic intensities in the junctions, also called the "hotspots" [197]. The SERS substrates are extremely sensitive and thus are prone to be contaminated by impurities. Impurities such as amorphous carbon, often a side product of laser-induced burning and degradation, have a huge scattering cross-section and can obscure the actual SERS spectra [177]. The leaching of ions from these NPs can cause toxicity in biological systems [198]. Nanoparticles such as silver, which has a high SERS enhancement capability, can be toxic to cells due to the generation of reactive oxygen species [199]. They also tend to denature proteins and cause pores in the cell membrane. Similarly, a few types of carbon nanomaterials can elicit harmful immune and non-immune responses in the human body and should be used with caution not to affect healthy cells [200]. Moreover, the transport of these nanoprobes to the target areas can be achieved by specific surface coatings or by invoking specialized release mechanisms commonly employed in the case of drug delivery.

Conclusions and Future Perspectives

The theranostic approach for treating diseases constitutes a system where the therapeutic and diagnostic modalities are integrated into a single system. This approach is challenging but promises to provide patient-tailored therapies and, most importantly, improve clinical outcomes. For successful disease management, choosing the appropriate theranostic tools is imperative. Fluorescence imaging, positron emission tomography, MRI, and CT are a few analytical techniques that have been used in theranostics. But using advanced multimodal spectroscopic tools and optical instruments has given theranostics a new direction. Spectroscopic techniques such as fluorescence and Raman spectroscopies have been combined with PTT to provide sufficient complementarity for seamless use. The emergence of RS as a part of the theranostic tool to determine minor biochemical variations across tissues and cells *in vivo* can diagnose fatal diseases. Such detection is now possible because of spectral fingerprint determination of biomolecules, the advanced variants of RS, and functional probes that have improved the spatial and temporal resolution of samples under investigation. A wide range of Raman probes, including plasmonic probes, metal oxide probes, carbon-based probes, etc., are used in diagnostics, facilitating single-molecule level detection and therapy options, offering rich structural information about cells and tissues without affecting the clinical outcome. Several of such prospective Raman-based probes that have been utilised or could be employed for various theranostic applications have been covered in this review. Numerous theranostic medicines based on nanoparticles have already been used in clinical trials, and many more are still in the pre-clinical stages. The use of RS and its sophisticated variants has the potential to push the limits of nanomedicine even further. They may create intelligent, adaptable theranostic platforms that will facilitate early diagnosis and treatment and help avert the onset of many fatal diseases.

Acknowledgments

Competing Interests

The authors have declared that no competing interest exists.

References

1. Warner S. Diagnostics + therapy = theranostics: strategy requires teamwork, partnering, and tricky regulatory maneuvering. The Scientist; 2004; 38-40.
2. Canetta E. Current and Future Advancements of Raman Spectroscopy Techniques in Cancer Nanomedicine. International journal of molecular sciences. 2021; 22: 13141.
3. Sung H, Ferlay J, Siegel R, Laversanne M, Soerjomataram I, Jemal A, et al. Global cancer statistics 2020: GLOBOCAN estimates of incidence and mortality worldwide for 36 cancers in 185 countries. Ca-a Cancer Journal For Clinicians. 2021; 71: 209-49.
4. Huang H, Lovell JF. Advanced functional nanomaterials for theranostics. Advanced functional materials. 2017; 27: 1603524.
5. Svenson S. Theranostics: Are We There Yet? Molecular Pharmaceutics. 2013; 10: 848-56.
6. Valm AM, Cohen S, Legant WR, Melunis J, Hershberg U, Wait E, et al. Applying systems-level spectral imaging and analysis to reveal the organelle interactome. Nature. 2017; 546: 162-7.
7. Choi KY, Liu G, Lee S, Chen X. Theranostic nanoplatforms for simultaneous cancer imaging and therapy: current approaches and future perspectives. Nanoscale. 2012; 4: 330-42.
8. Auner GW, Koya SK, Huang C, Broadbent B, Trexler M, Auner Z, et al. Applications of Raman spectroscopy in cancer diagnosis. Cancer and Metastasis Reviews. 2018; 37: 691-717.
9. Adams WR, Mehl B, Lieser E, Wang M, Patton S, Throckmorton GA, et al. Multi-modal nonlinear optical and thermal imaging platform for label-free characterization of biological tissue. Scientific reports. 2021; 11: 1-13.
10. You S, Tu H, Chaney EJ, Sun Y, Zhao Y, Bower AJ, et al. Intravital imaging by simultaneous label-free autofluorescence-multiharmonic microscopy. Nature communications. 2018; 9: 1-9.
11. Miller L, Wang Q, Telivala T, Smith R, Lanzirotti A, Miklossy J. Synchrotron-based infrared and X-ray imaging shows focalized accumulation of Cu and Zn co-localized with beta-amyloid deposits in Alzheimer's disease. Journal of Structural Biology. 2006; 155: 30-7.
12. Szczerbowska-Boruchowska M, Dumas P, Kastyak M, Chwiej J, Lankosz M, Adamek D, et al. Biomolecular investigation of human substantia nigra in Parkinson's disease by synchrotron radiation Fourier transform infrared micro spectroscopy. Archives of Biochemistry and Biophysics. 2007; 459: 241-8.
13. D'Acunto M, Gaeta R, Capanna R, Franchi A. Contribution of Raman Spectroscopy to Diagnosis and Grading of Chondrogenic Tumors. Scientific Reports. 2020; 10: 1-12.
14. Ishigaki M, Maeda Y, Taketani A, Andriana B, Ishihara R, Wongravee K, et al. Diagnosis of early-stage esophageal cancer by Raman spectroscopy and chemometric techniques. Analyst. 2016; 141: 1027-33.
15. Turrell G, Corset J. Raman microscopy: developments and applications: Academic Press; 1996.
16. Zumbusch A, Holtom GR, Xie XS. Three-dimensional vibrational imaging by coherent anti-Stokes Raman scattering. Physical review letters. 1999; 82: 4142.
17. Leproux P, Couderc V, De Angelis A, Okuno M, Kano H, Hamaguchi H-o. New opportunities offered by compact sub-nanosecond supercontinuum sources in ultra-broadband multiplex CARS microspectroscopy. Journal of Raman Spectroscopy. 2011; 42: 1871-4.
18. Freudiger CW, Min W, Saar BG, Lu S, Holtom GR, He C, et al. Label-free biomedical imaging with high sensitivity by stimulated Raman scattering microscopy. Science. 2008; 322: 1857-61.
19. Raman CV, Krishnan KS. A new type of secondary radiation. Nature; 1928; 121: 501-502.
20. Matousek P, Stone N. Development of deep subsurface Raman spectroscopy for medical diagnosis and disease monitoring. Chemical Society Reviews. 2016; 45: 1794-1802.
21. Matousek P, Clark IP, Draper ERC, Morris MD, Goodship AE, Everall N, et al. Subsurface probing in diffusely scattering media using spatially offset Raman spectroscopy. Applied spectroscopy. 2005; 59: 393-400.
22. Kneipp K, Ozaki Y, Tian Z-Q. Recent Developments In Plasmon-supported Raman Spectroscopy: 45 Years Of Enhanced Raman Signals: World Scientific Publishing Europe Ltd., London, 2017.
23. Zong C, Xu M, Xu L-J, Wei T, Ma X, Zheng X-S, et al. Surface-enhanced Raman spectroscopy for bioanalysis: reliability and challenges. Chemical reviews. 2018; 118: 4946-80.

24. Alessandri I, Lombardi JR. Enhanced Raman scattering with dielectrics. Chemical reviews. 2016; 116: 14921-81.

25. Willets KA, Van Duyne RP. Localized surface plasmon resonance spectroscopy and sensing. Annu Rev Phys Chem. 2007; 58: 267-97.

26. Vo-Dinh T. Nanobiosensing using plasmonic nanoprobes. Ieee Journal of Selected Topics in Quantum Electronics. 2008; 14: 198-205.

27. Wang H, Vo-Dinh T. Plasmonic Coupling Interference (PCI) Nanoprobes for Nucleic Acid Detection. Small. 2011; 7: 3067-74.

28. Yuan Y, Raj P, Zhang J, Siddhanta S, Barman I, Bulte JWM. Furin-Mediated Self-Assembly of Olsalazine Nanoparticles for Targeted Raman Imaging of Tumors. Angewandte Chemie. 2021; 133: 3969-73.

29. Khan ZU, Khan A, Chen YM, Shah NS, Muhammad N, Khan AU, et al. Biomedical applications of green synthesized Nobel metal nanoparticles. Journal of Photochemistry and Photobiology B-Biology. 2017; 173: 150-64.

30. Xie W, Qiu PH, Mao CB. Bio-imaging, detection and analysis by using nanostructures as SERS substrates. Journal of Materials Chemistry. 2011; 21: 5190-202.

31. Conde J, Bao C, Cui D, Baptista P, Tian F. Antibody-drug gold nanoantennas with Raman spectroscopic fingerprints for *in vivo* tumour theranostics. Journal of Controlled Release. 2014; 183: 87-93.

32. Xavier J, Vincent S, Meder F, Vollmer F. Advances in optoplasmonic sensors - combining optical nano/microcavities and photonic crystals with plasmonic nanostructures and nanoparticles. Nanophotonics. 2018; 7: 1-38.

33. Zhu S, Xu G. Single-walled carbon nanohorns and their applications. Nanoscale. 2010; 2: 2538-49.

34. Guerra J, Herrero M, Vazquez E. Carbon nanohorns as alternative gene delivery vectors. Rsc Advances. 2014; 4: 27315-21.

35. Huang H, Lovell J. Advanced Functional Nanomaterials for Theranostics. Advanced Functional Materials. 2017; 27: 1603524.

36. Meier M, Wokaun A, Vo-Dinh T. Silver particles on stochastic quartz substrates providing tenfold increase in raman enhancement. Journal of Physical Chemistry. 1985; 89: 1843-6.

37. Vo-Dinh T, Uziel M, Morrison AL. Surface-enhanced Raman analysis of benzo [a] pyrene-DNA adducts on silver-coated cellulose substrates. Applied spectroscopy. 1987; 41: 605-10.

38. Vo-Dinh T. Surface-enhanced Raman spectroscopy using metallic nanostructures. TrAC Trends in Analytical Chemistry. 1998; 17: 557-82.

39. Wabuyele MB, Vo-Dinh T. Detection of human immunodeficiency virus type 1 DNA sequence using plasmonics nanoprobes. Analytical chemistry. 2005; 77: 7810-5.

40. Siddhanta S, Narayana C. Surface Enhanced Raman Spectroscopy of Proteins: Implications for Drug Designing Invited Review Article. Nanomaterials and Nanotechnology. 2012; 2: 1-13.

41. Siddhanta S, Thakur V, Narayana C, Shivaprasad S. Universal Metal-Semiconductor Hybrid Nanostructured SERS Substrate for Biosensing. ACS Applied Materials & Interfaces. 2012; 4: 5807-12.

42. Zhang X, Ge Y, Liu M, Pei Y, He P, Song W, et al. DNA-Au Janus Nanoparticles for *In situ* SERS Detection and Targeted Chemo-photodynamic Synergistic Therapy. Analytical Chemistry. 2022; 94: 7823-32.

43. Cai W, Gao T, Hong H, Sun J. Applications of gold nanoparticles in cancer nanotechnology. Nanotechnology, science and applications. 2008; 1: 17-32.

44. Li Y, Wei Q, Ma F, Li X, Liu F, Zhou M. Surface-enhanced Raman nanoparticles for tumor theranostics applications. Acta Pharmaceutica Sinica B. 2018; 8: 349-59.

45. Scotter CNG. Non-destructive spectroscopic techniques for the measurement of food quality. Trends in food science & technology. 1997; 8: 285-92.

46. Born M, Wolf E. Principles of optics: electromagnetic theory of propagation, interference and diffraction of light: Elsevier; 2013.

47. Lin L, Bi X, Gu Y, Wang F, Ye J. Surface-enhanced Raman scattering nanotags for bioimaging. Journal of Applied Physics. 2021; 129: 191101.

48. Colthup N. Introduction to infrared and Raman spectroscopy: Elsevier; 2012.

49. Song L-MWK, Marcon NE. Fluorescence and Raman spectroscopy. Gastrointestinal Endoscopy Clinics. 2003; 13: 279-96.

50. Hoehse M, Gornushkin I, Merk S, Panne U. Assessment of suitability of diode pumped solid state lasers for laser induced breakdown and Raman spectroscopy. Journal of analytical atomic spectrometry. 2011; 26: 414-24.

51. Carey PR. Raman and resonance Raman spectroscopy. New Comprehensive Biochemistry: Elsevier; 1985; 11: 27-64.

52. Yang Z, Aizpurua J, Xu H. Electromagnetic field enhancement in TERS configurations. Journal of Raman Spectroscopy. 2009; 40: 1343-8.

53. Schatz GC, Young MA, Duyne RPV. Electromagnetic mechanism of SERS. Surface-enhanced Raman scattering: Springer; 2006; 103: 19-45.

54. Paidi S, Siddhanta S, Strouse R, McGivney J, Larkin C, Barman I. Rapid Identification of Biotherapeutics with Label-Free Raman Spectroscopy. Analytical Chemistry. 2016; 88: 4361-8.

55. Fleischmann PJ. Hendra, and AJ McQuillan. Chem Phys Lett. 1974; 26: 163.

56. Perez-Jimenez A, Lyu D, Lu Z, Liu G, Ren R. Surface-enhanced Raman spectroscopy: benefits, trade-offs and future developments. Chemical Science. 2020; 11: 4563-77.

57. Ji W, Kitahama Y, Xue X, Zhao B, Ozaki Y. Generation of pronounced resonance profile of charge-transfer contributions to surface-enhanced Raman scattering. The Journal of Physical Chemistry C. 2012; 116: 2515-20.

58. Trügler A, Tinguely J-C, Jakopic G, Hohenester U, Krenn JR, Hohenau A. Near-field and SERS enhancement from rough plasmonic nanoparticles. Physical Review B. 2014; 89: 165409.

59. Mai QD, Nguyen HA, Phung TLH, Xuan Dinh N, Tran QH, Doan TQ, et al. Silver Nanoparticles-Based SERS Platform towards Detecting Chloramphenicol and Amoxicillin: An Experimental Insight into the Role of HOMO–LUMO Energy Levels of the Analyte in the SERS Signal and Charge Transfer Process. The Journal of Physical Chemistry C. 2022; 126: 7778-90.

60. Pilot R, Signorini R, Durante C, Orian L, Bhamidipati M, Fabris L. A Review on Surface-Enhanced Raman Scattering. Biosensors-Basel. 2019; 9: 57.

61. Liao PF, Wokaun A. Lightning rod effect in surface enhanced Raman scattering. The Journal of Chemical Physics. 1982; 76: 751-2.

62. Moskovits M. Surface-enhanced spectroscopy. Reviews of modern physics. 1985; 57: 783.

63. Gersten J, Nitzan A. Electromagnetic theory of enhanced raman-scattering by molecules adsorbed on rough surfaces. Journal of Chemical Physics. 1980; 73: 3023-37.

64. Naqvi T, Bajpai A, Bharati M, Kulkarni M, Siddiqui A, Soma V, et al. Ultra-sensitive reusable SERS sensor for multiple hazardous materials detection on single platform. Journal of Hazardous Materials. 2021; 407: 124353.

65. Myakalwar A, Sreedhar S, Barman I, Dingari N, Rao S, Kiran P, et al. Laser-induced breakdown spectroscopy-based investigation and classification of pharmaceutical tablets using multivariate chemometric analysis. Talanta. 2011; 87: 53-9.

66. Xu K, Zhou R, Takei K, Hong M. Toward flexible surface-enhanced Raman scattering (SERS) sensors for point-of-care diagnostics. Advanced Science. 2019; 6: 1900925.

67. Huang Z, Siddhanta S, Zheng G, Kickler T, Barman I. Rapid, Label-free Optical Spectroscopy Platform for Diagnosis of Heparin-Induced Thrombocytopenia. Angewandte Chemie International Edition. 2020; 59: 5972-8.

68. Wu L, Dias A, Dieguez L. Surface enhanced Raman spectroscopy for tumor nucleic acid: Towards cancer diagnosis and precision medicine. Biosensors & Bioelectronics. 2022; 204: 114075.

69. Noonan J, Asiala S, Grassia G, MacRitchie N, Gracie K, Carson J, et al. *In vivo* multiplex molecular imaging of vascular inflammation using surface-enhanced Raman spectroscopy. Theranostics. 2018; 8: 6195-209.

70. Robert B. Resonance raman spectroscopy. Photosynthesis research. 2009; 101: 147-55.

71. Kakita M, Kaliaperumal V, Hamaguchi H. Resonance Raman quantification of the redox state of cytochromes b and c in-vivo and in-vitro. Journal of Biophotonics. 2012; 5: 20-4.

72. Merlin JC. Resonance Raman spectroscopy of carotenoids and carotenoid-containing systems. Pure and Applied Chemistry. 1985; 57: 785-92.

73. Tintchev F, Kuhlmann U, Wackerbarth H, Töpfl S, Heinz V, Knorr D, et al. Redox processes in pressurised smoked salmon studied by resonance Raman spectroscopy. Food chemistry. 2009; 112: 482-6.

74. Rich C, McHale J. Resonance Raman Spectra of Individual Excitonically Coupled Chromophore Aggregates. Journal of Physical Chemistry C. 2013; 117: 10856-65.

75. Schellenberg P, Johnson E, Esposito A, Reid P, Parson W. Resonance Raman scattering by the green fluorescent protein and an analogue of its chromophore. Journal of Physical Chemistry B. 2001; 105: 5316-22.

76. Zavaleta CL, Hartman KB, Miao Z, James ML, Kempen P, Thakor AS, et al. Preclinical evaluation of Raman nanoparticle biodistribution for their potential use in clinical endoscopy imaging. Small. 2011; 7: 2232-40.

77. Harada Y, Takamatsu T. Raman molecular imaging of cells and tissues: towards functional diagnostic imaging without labeling. Current Pharmaceutical Biotechnology. 2013; 14: 133-40.

78. Kendall C, Stone N, Shepherd N, Geboes K, Warren B, Bennett R, et al. Raman spectroscopy, a potential tool for the objective identification and classification of neoplasia in Barrett's oesophagus. The Journal of

Pathology: A Journal of the Pathological Society of Great Britain and Ireland. 2003; 200: 602-9.

79. Almond LM, Hutchings J, Lloyd G, Barr H, Shepherd N, Day J, et al. Endoscopic Raman spectroscopy enables objective diagnosis of dysplasia in Barrett's esophagus. Gastrointestinal endoscopy. 2014; 79: 37-45.

80. Lakshmi R, Alexander M, Kurien J, Mahato K, Kartha V. Osteoradionecrosis (ORN) of the mandible: A laser Raman spectroscopic study. Applied Spectroscopy. 2003; 57: 1100-16.

81. Vidyasagar M, Maheedhar K, Vadhiraja B, Fernendes D, Kartha V, Krishna C. Prediction of radiotherapy response in cervix cancer by Raman spectroscopy: A pilot study. Biopolymers. 2008; 89: 530-7.

82. Gong B, Oest ME, Mann KA, Damron TA, Morris MD. Raman spectroscopy demonstrates prolonged alteration of bone chemical composition following extremity localized irradiation. Bone. 2013; 57: 252-8.

83. Barth A, Zscherp C. What vibrations tell about proteins. Quarterly reviews of biophysics. 2002; 35: 369-430.

84. Cao L, Fernando K, Liang W, Seilkop A, Veca L, Sun Y, et al. Carbon dots for energy conversion applications. Journal of Applied Physics. 2019; 125.

85. Tilmaciu C, Morris M. Carbon nanotube biosensors. Frontiers in Chemistry. 2015; 3: 59.

86. Cheng M, Prabakaran P, Kumar R, Sridhar S, Ebong E. Synthesis of Functionalized 10-nm Polymer-coated Gold Particles for Endothelium Targeting and Drug Delivery. Jove-Journal of Visualized Experiments. 2018; 131: e56760.

87. Ko KH, Kown C-I, Park JM, Lee HG, Han NY, Hahm KB. Molecular imaging for theranostics in gastroenterology: one stone to kill two birds. Clinical Endoscopy. 2014; 47: 383-88.

88. Zavaleta CL, Smith BR, Walton I, Doering W, Davis G, Shojaei B, et al. Multiplexed imaging of surface enhanced Raman scattering nanotags in living mice using noninvasive Raman spectroscopy. Proceedings of the National Academy of Sciences. 2009; 106: 13511-6.

89. Palonpon AF, Sodeoka M, Fujita K. Molecular imaging of live cells by Raman microscopy. Current opinion in chemical biology. 2013; 17: 708-15.

90. Horgan C, Bergholt M, Nagelkerke A, Thin M, Pence I, Kauscher U, et al. Integrated photodynamic Raman theranostic system for cancer diagnosis, treatment, and post-treatment molecular monitoring. Theranostics. 2021; 11: 2006-19.

91. Shamjith S, Joseph M, Murali V, Remya G, Nair J, Suresh C, et al. NADH-depletion triggered energy shutting with cyclometalated iridium (III) complex enabled bimodal Luminescence-SERS sensing and photodynamic therapy. Biosensors & Bioelectronics. 2022; 204: 114087.

92. Joseph M, Ramya A, Vijayan V, Nair J, Bastian B, Pillai R, et al. Targeted Theranostic Nano Vehicle Endorsed with Self-Destruction and Immunostimulatory Features to Circumvent Drug Resistance and Wipe-Out Tumor Reinitiating Cancer Stem Cells. Small. 2020; 16: 2003309.

93. Jiang Y, Pu K. Molecular Probes for Autofluorescence-Free Optical Imaging. Chemical Reviews. 2021; 121: 13086-131.

94. He C, Zhu J, Zhang H, Qiao R, Zhang R. Photoacoustic Imaging Probes for Theranostic Applications. Biosensors-Basel. 2022; 12: 947.

95. Yang R, Gao Y, Ouyang Z, Shi X, Shen M. Gold nanostar-based complexes applied for cancer theranostics. View. 2022: 20200171.

96. Ricciardi L, La Deda M. Recent advances in cancer photo-theranostics: the synergistic combination of transition metal complexes and gold nanostructures. SN Applied Sciences. 2021; 3: 372.

97. Ko C-N, Li G, Leung C-H, Ma D-L. Dual function luminescent transition metal complexes for cancer theranostics: The combination of diagnosis and therapy. Coordination Chemistry Reviews. 2019; 381: 79-103.

98. Ma D-L, Wu C, Li G, Yung T-L, Leung C-H. Transition metal complexes as imaging or therapeutic agents for neurodegenerative diseases. Journal of Materials Chemistry B. 2020; 8: 4715-25.

99. Liu C, Zhang R, Zhang W, Liu J, Wang Y-L, Du Z, et al. "Dual-key-and-lock" ruthenium complex probe for lysosomal formaldehyde in cancer cells and tumors. Journal of the American Chemical Society. 2019; 141: 8462-72.

100. Meng X, Zhang J, Sun Z, Zhou L, Deng G, Li S, et al. Hypoxia-triggered single molecule probe for high-contrast NIR II/PA tumor imaging and robust photothermal therapy. Theranostics. 2018; 8: 6025-34.

101. Meng X, Yang Y, Zhou L, Zhang L, Lv Y, Li S, et al. Dual-Responsive Molecular Probe for Tumor Targeted Imaging and Photodynamic Therapy. Theranostics. 2017; 7: 1781-94.

102. He H, Zhang X, Du L, Ye M, Lu Y, Xue J, et al. Molecular imaging nanoprobes for theranostic applications. Advanced Drug Delivery Reviews. 2022; 186: 114320.

103. Patel K, Singh R, Kim H. Carbon-based nanomaterials as an emerging platform for theranostics. Materials Horizons. 2019; 6: 434-69.

104. Liu Z, Tabakman S, Welsher K, Dai H. Carbon Nanotubes in Biology and Medicine: *In vitro* and *in vivo* Detection, Imaging and Drug Delivery. Nano Research. 2009; 2: 85-120.

105. Panwar N, Soehartono A, Chan K, Zeng S, Xu G, Qu J, et al. Nanocarbons for Biology and Medicine: Sensing, Imaging, and Drug Delivery. Chemical Reviews. 2019; 119: 9559-656.

106. Guerra J, Herrero MA, Vázquez E. Carbon nanohorns as alternative gene delivery vectors. RSC advances. 2014; 4: 27315-21.

107. Tang L, Xiao Q, Mei Y, He S, Zhang Z, Wang R, et al. Insights on functionalized carbon nanotubes for cancer theranostics. Journal of Nanobiotechnology. 2021; 19: 1-28.

108. Robinson J, Welsher K, Tabakman S, Sherlock S, Wang H, Luong R, et al. High Performance *In vivo* Near-IR (> 1 mu m) Imaging and Photothermal Cancer Therapy with Carbon Nanotubes. Nano Research. 2010; 3: 779-93.

109. Kim S, Lee Y, Lee J, Hong J, Khang D. PEGylated anticancer-carbon nanotubes complex targeting mitochondria of lung cancer cells. Nanotechnology. 2017; 28: 465102.

110. Bhirde A, Liu G, Jin A, Iglesias-Bartolome R, Sousa A, Leapman R, et al. Combining Portable Raman Probes with Nanotubes for Theranostic Applications. Theranostics. 2011; 1: 310-21.

111. Bhirde AA, Liu G, Jin A, Iglesias-Bartolome R, Sousa AA, Leapman RD, et al. Combining portable Raman probes with nanotubes for theranostic applications. Theranostics. 2011; 1: 310.

112. Nergiz S, Gandra N, Tadepalli S, Singamaneni S. Multifunctional Hybrid Nanopatches of Graphene Oxide and Gold Nanostars for Ultraefficient Photothermal Cancer Therapy. ACS Applied Materials & Interfaces. 2014; 6: 16395-402.

113. Ingle T, Dervishi E, Biris A, Mustafa T, Buchanan R, Biris A. Raman spectroscopy analysis and mapping the biodistribution of inhaled carbon nanotubes in the lungs and blood of mice. Journal of Applied Toxicology. 2013; 33: 1044-52.

114. Song J, Wang F, Yang X, Ning B, Harp M, Culp S, et al. Gold Nanoparticle Coated Carbon Nanotube Ring with Enhanced Raman Scattering and Photothermal Conversion Property for Theranostic Applications. Journal of the American Chemical Society. 2016; 138: 7005-15.

115. Beqa L, Fan Z, Singh A, Senapati D, Ray P. Gold Nano-Popcorn Attached SWCNT Hybrid Nanomaterial for Targeted Diagnosis and Photothermal Therapy of Human Breast Cancer Cells. ACS Applied Materials & Interfaces. 2011; 3: 3316-24.

116. Taylor R, Lee T, Scherman O, Esteban R, Aizpurua J, Huang F, et al. Precise Subnanometer Plasmonic Junctions for SERS within Gold Nanoparticle Assemblies Using Cucurbit[n]uril "Glue". ACS Nano. 2011; 5: 3878-87.

117. Boisselier E, Astruc D. Gold nanoparticles in nanomedicine: preparations, imaging, diagnostics, therapies and toxicity. Chemical Society Reviews. 2009; 38: 1759-82.

118. Yuan Y, Zhang J, Qi X, Li S, Liu G, Siddhanta S, et al. Furin-mediated intracellular self-assembly of olsalazine nanoparticles for enhanced magnetic resonance imaging and tumour therapy. Nature Materials. 2019; 18: 1376-1383.

119. Liu H, Gao X, Xu C, Liu D. SERS Tags for Biomedical Detection and Bioimaging. Theranostics. 2022; 12: 1870-903.

120. Gong T, Das C, Yin M, Lv T, Singh N, Soehartono A, et al. Development of SERS tags for human diseases screening and detection. Coordination Chemistry Reviews. 2022; 470: 214711.

121. Li P, Long F, Chen W, Chen J, Chu P, Wang H. Fundamentals and applications of surface-enhanced Raman spectroscopy-based biosensors. Current Opinion in Biomedical Engineering. 2020; 13: 51-9.

122. Yan M, Li H, Li M, Cao X, She Y, Chen Z. Advances in Surface-Enhanced Raman Scattering-Based Aptasensors for Food Safety Detection. Journal of Agricultural and Food Chemistry. 2021; 69: 14049-64.

123. Kim M, Lee J, Nam J. Plasmonic Photothermal Nanoparticles for Biomedical Applications. Advanced Science. 2019; 6: 1900471.

124. Zavaleta C, Garai E, Liu J, Sensarn S, Mandella M, Van de Sompel D, et al. A Raman-based endoscopic strategy for multiplexed molecular imaging. Proceedings of the National Academy of Sciences of the United States of America. 2013; 110: E2288-E97.

125. Jokerst J, Cole A, Van de Sompel D, Gambhir S. Gold Nanorods for Ovarian Cancer Detection with Photoacoustic Imaging and Resection Guidance via Raman Imaging in Living Mice. ACS Nano. 2012; 6: 10366-77.

126. Liang L, Zheng C, Zhang H, Xu S, Zhang Z, Hu C, et al. Exploring type II microcalcifications in benign and premalignant breast lesions by shell-isolated nanoparticle-enhanced Raman spectroscopy (SHINERS). Spectrochimica Acta Part a-Molecular and Biomolecular Spectroscopy. 2014; 132: 397-402.

127. Zheng C, Liang L, Xu S, Zhang H, Hu C, Bi L, et al. The use of Au@SiO2 shell-isolated nanoparticle-enhanced Raman spectroscopy for human breast cancer detection. Analytical and Bioanalytical Chemistry. 2014; 406: 5425-32.

128. Mert S, Ozbek E, Otunctemur A, Culha M. Kidney tumor staging using surface-enhanced Raman scattering. Journal of Biomedical Optics. 2015; 20: 047002.

129. Feng S, Li Z, Chen G, Lin D, Huang S, Huang Z, et al. Ultrasound-mediated method for rapid delivery of nano-particles into cells for intracellular surface-enhanced Raman spectroscopy and cancer cell screening. Nanotechnology. 2015; 26: 065101.

130. Lin D, Feng S, Pan J, Chen Y, Lin J, Chen G, et al. Colorectal cancer detection by gold nanoparticle based surface-enhanced Raman spectroscopy of blood serum and statistical analysis. Optics Express. 2011; 19: 13565-77.

131. Feng S, Chen R, Lin J, Pan J, Wu Y, Li Y, et al. Gastric cancer detection based on blood plasma surface-enhanced Raman spectroscopy excited by polarized laser light. Biosensors & Bioelectronics. 2011; 26: 3167-74.

132. Feng S, Pan J, Wu Y, Lin D, Chen Y, Xi G, et al. Study on gastric cancer blood plasma based on surface-enhanced Raman spectroscopy combined with multivariate analysis. Science China-Life Sciences. 2011; 54: 828-34.

133. Ito H, Inoue H, Hasegawa K, Hasegawa Y, Shimizu T, Kimura S, et al. Use of surface-enhanced Raman scattering for detection of cancer-related serum-constituents in gastrointestinal cancer patients. Nanomedicine-Nanotechnology Biology and Medicine. 2014; 10: 599-608.

134. Del Mistro G, Cervo S, Mansutti E, Spizzo R, Colombatti A, Belmonte P, et al. Surface-enhanced Raman spectroscopy of urine for prostate cancer detection: a preliminary study. Analytical and Bioanalytical Chemistry. 2015; 407: 3271-5.

135. Kneipp K, Haka A, Kneipp H, Badizadegan K, Yoshizawa N, Boone C, et al. Surface-enhanced Raman Spectroscopy in single living cells using gold nanoparticles. Applied Spectroscopy. 2002; 56: 150-4.

136. Cottat M, D'Andrea C, Yasukuni R, Malashikhina N, Grinyte R, Lidgi-Guigui N, et al. High Sensitivity, High Selectivity SERS Detection of MnSOD Using Optical Nanoantennas Functionalized with Aptamers. Journal of Physical Chemistry C. 2015; 119: 15532-40.

137. Chundayil Madathil G, Iyer S, Thankappan K, Gowd GS, Nair S, Koyakutty M. A novel surface enhanced Raman catheter for rapid detection, classification, and grading of oral cancer. Advanced healthcare materials. 2019; 8: 1801557.

138. Zong S, Wang Z, Chen H, Yang J, Cui Y. Surface Enhanced Raman Scattering Traceable and Glutathione Responsive Nanocarrier for the Intracellular Drug Delivery. Analytical Chemistry. 2013; 85: 2223-30.

139. Liu X, Tao H, Yang K, Zhang S, Lee S, Liu Z. Optimization of surface chemistry on single-walled carbon nanotubes for *in vivo* photothermal ablation of tumors. Biomaterials. 2011; 32: 144-51.

140. Qian X, Peng X, Ansari D, Yin-Goen Q, Chen G, Shin D, et al. *In vivo* tumor targeting and spectroscopic detection with surface-enhanced Raman nanoparticle tags. Nature Biotechnology. 2008; 26: 83-90.

141. Zhang W, Wang Y, Sun X, Wang W, Chen L. Mesoporous titania based yolk-shell nanoparticles as multifunctional theranostic platforms for SERS imaging and chemo-photothermal treatment. Nanoscale. 2014; 6: 14514-22.

142. Gong B, Shen Y, Li H, Li X, Huan X, Zhou J, et al. Thermo-responsive polymer encapsulated gold nanorods for single continuous wave laser-induced photodynamic/photothermal tumour therapy. Journal of Nanobiotechnology. 2021; 19: 1-14.

143. Garai E, Sensarn S, Zavaleta C, Loewke N, Rogalla S, Mandella M, et al. A Real-Time Clinical Endoscopic System for Intraluminal, Multiplexed Imaging of Surface-Enhanced Raman Scattering Nanoparticles. Plos One. 2015; 10: e0123185.

144. Kircher M, de la Zerda A, Jokerst J, Zavaleta C, Kempen P, Mittra E, et al. A brain tumor molecular imaging strategy using a new triple-modality MRI-photoacoustic-Raman nanoparticle. Nature Medicine. 2012; 18: 829-834.

145. Davis R, Kiss B, Trivedi D, Metzner T, Liao J, Gambhir S. Surface-Enhanced Raman Scattering Nanoparticles for Multiplexed Imaging of Bladder Cancer Tissue Permeability and Molecular Phenotype. ACS Nano. 2018; 12: 9669-79.

146. DeRosa M, Crutchley R. Photosensitized singlet oxygen and its applications. Coordination Chemistry Reviews. 2002; 233: 351-71.

147. Feng J, Chen L, Xia Y, Xing J, Li Z, Qian Q, et al. Bioconjugation of gold nanobipyramids for SERS detection and targeted photothermal therapy in breast cancer. ACS Biomaterials Science & Engineering. 2017; 3: 608-18.

148. Chang Y, Gao H, Zhang N, Tao X, Sun T, Zhang J, et al. Synergistic Reducing Effect for Synthesis of Well-Defined Au Nanooctopods With Ultra-Narrow Plasmon Band Width and High Photothermal Conversion Efficiency. Frontiers in Chemistry. 2018; 6: 335.

149. Andreiuk B, Nicolson F, Clark LM, Panikkanvalappil SR, Kenry, Rashidian M, et al. Design and synthesis of gold nanostars-based SERS nanotags for bioimaging applications. Nanotheranostics. 2022; 6: 10-30.

150. Zhang Y, Qian J, Wang D, Wang Y, He S. Multifunctional Gold Nanorods with Ultrahigh Stability and Tunability for *In vivo* Fluorescence Imaging, SERS Detection, and Photodynamic Therapy. Angewandte Chemie-International Edition. 2013; 52: 1148-51.

151. Jokerst J, Gambhir S. Molecular Imaging with Theranostic Nanoparticles. Accounts of Chemical Research. 2011; 44: 1050-60.

152. Keren S, Zavaleta C, Cheng Z, de la Zerda A, Gheysens O, Gambhir S. Noninvasive molecular imaging of small living subjects using Raman spectroscopy. Proceedings of the National Academy of Sciences of the United States of America. 2008; 105: 5844-9.

153. Ren E, Zhang C, Li D, Pang X, Liu G. Leveraging metal oxide nanoparticles for bacteria tracing and eradicating. View. 2020; 1: 20200052.

154. Yamada H, Yamamoto Y. Surface enhanced raman-scattering (sers) of chemisorbed species on various kinds of metals and semiconductors. Surface Science. 1983; 134: 71-90.

155. Han X, Ji W, Zhao B, Ozaki Y. Semiconductor-enhanced Raman scattering: active nanomaterials and applications. Nanoscale. 2017; 9: 4847-61.

156. Shan Y, Zheng Z, Liu J, Yang Y, Li Z, Huang Z, et al. Niobium pentoxide: a promising surface-enhanced Raman scattering active semiconductor substrate. Npj Computational Materials. 2017; 3: 11.

157. Sharma A, Saini A, Kumar N, Tejwan N, Singh T, Thakur V, et al. Methods of preparation of metal-doped and hybrid tungsten oxide nanoparticles for anticancer, antibacterial, and biosensing applications. Surfaces and Interfaces. 2022; 28: 101641.

158. Lin J, Ma X, Li A, Akakuru OU, Pan C, He M, et al. Multiple Valence States of Fe Boosting SERS Activity of Fe3O4 Nanoparticles and Enabling Effective SERS-MRI Bimodal Cancer Imaging. Fundamental Research. 2022. https://doi.org/10.1016/j.fmre.2022.04.018

159. Han J, Tian Y, Wang M, Li Y, Yin J, Qu W, et al. Proteomics unite traditional toxicological assessment methods to evaluate the toxicity of iron oxide nanoparticles. Front Pharmacol. 2022; 13: 1011065.

160. Abedin M, Umapathi S, Mahendrakar H, Laemthong T, Coleman H, Muchangi D, et al. Polymer coated gold-ferric oxide superparamagnetic nanoparticles for theranostic applications. Journal of Nanobiotechnology. 2018; 16: 1-13.

161. Rissi N, Comparetti E, Estevao B, Mastelaro V, Zucolotto V. Doped Plasmonic Zinc Oxide Nanoparticles with Near-Infrared Absorption for Antitumor Activity. ACS Applied Nano Materials. 2021; 4: 9779-89.

162. Xiao X, Liang S, Zhao Y, Huang D, Xing B, Cheng Z, et al. Core–shell structured 5-FU@ ZIF-90@ ZnO as a biodegradable nanoplatform for synergistic cancer therapy. Nanoscale. 2020; 12: 3846-54.

163. Han Y, Lei S, Lu J, He Y, Chen Z, Ren L, et al. Potential use of SERS-assisted theranostic strategy based on Fe3O4/Au cluster/shell nanocomposites for bio-detection, MRI, and magnetic hyperthermia. Materials Science and Engineering C-Materials For Biological Applications. 2016; 64: 199-207.

164. Schneider-Futschik E, Reyes-Ortega F. Advantages and Disadvantages of Using Magnetic Nanoparticles for the Treatment of Complicated Ocular Disorders. Pharmaceutics. 2021; 13: 1157.

165. Hajba L, Guttman A. The use of magnetic nanoparticles in cancer theranostics: Toward handheld diagnostic devices. Biotechnology Advances. 2016; 34: 354-61.

166. Jibin K, Victor M, Saranya G, Santhakumar H, Murali V, Maiti KK, et al. Nanohybrids of magnetically intercalated optical metamaterials for magnetic resonance/Raman imaging and *in situ* chemodynamic/photothermal therapy. ACS applied bio materials. 2021; 4: 5742-52.

167. Jin R, Lin B, Li D, Ai H. Superparamagnetic iron oxide nanoparticles for MR imaging and therapy: design considerations and clinical applications. Current Opinion in Pharmacology. 2014; 18: 18-27.

168. Fonovic M, Bogyo M. Activity-based probes as a tool for functional proteomic analysis of proteases. Expert Review of Proteomics. 2008; 5: 721-30.

169. Ben-Nun Y, Merquiol E, Brandis A, Turk B, Scherz A, Blum G. Photodynamic Quenched Cathepsin Activity Based Probes for Cancer Detection and Macrophage Targeted Therapy. Theranostics. 2015; 5: 847-62.

170. Paidi S, Rizwan A, Zheng C, Cheng M, Glunde K, Barman I. Label-Free Raman Spectroscopy Detects Stromal Adaptations in Premetastatic Lungs Primed by Breast Cancer. Cancer Research. 2017; 77: 247-56.

171. Downes A, Elfick A. Raman Spectroscopy and Related Techniques in Biomedicine. Sensors. 2010; 10: 1871-89.

172. Nakashima S. Raman imaging of semiconductor materials: characterization of static and dynamic properties. Journal of Physics-Condensed Matter. 2004; 16: S25-S37.
173. Jermyn M, Desroches J, Aubertin K, St-Arnaud K, Madore W, De Montigny E, et al. A review of Raman spectroscopy advances with an emphasis on clinical translation challenges in oncology. Physics in Medicine and Biology. 2016; 61: R370-R400.
174. Aoki PHB, Furini LN, Alessio P, Aliaga AE, Constantino CJL. Surface-enhanced Raman scattering (SERS) applied to cancer diagnosis and detection of pesticides, explosives, and drugs. Reviews in Analytical Chemistry. 2013; 32: 55-76.
175. McNay G, Eustace D, Smith W, Faulds K, Graham D. Surface-Enhanced Raman Scattering (SERS) and Surface-Enhanced Resonance Raman Scattering (SERRS): A Review of Applications. Applied Spectroscopy. 2011; 65: 825-37.
176. Mai Q, Nguyen H, Phung T, Dinh N, Tran Q, Doan T, et al. Photoinduced Enhanced Raman Spectroscopy for the Ultrasensitive Detection of a Low-Cross-Section Chemical, Urea, Using Silver-Titanium Dioxide Nanostructures. ACS Applied Nano Materials. 2022; 5: 15518-30.
177. Eberhardt K, Stiebing C, Matthaus C, Schmitt M, Popp J. Advantages and limitations of Raman spectroscopy for molecular diagnostics: an update. Expert Review of Molecular Diagnostics. 2015; 15: 773-87.
178. Mao P, Liu C, Favraud G, Chen Q, Han M, Fratalocchi A, et al. Broadband single molecule SERS detection designed by warped optical spaces. Nature Communications. 2018; 9.
179. Zhang Y, Lin L, He J, Ye J. Optical penetration of surface-enhanced micro-scale spatial offset Raman spectroscopy in turbid gel and biological tissue. Journal of Innovative Optical Health Sciences. 2021; 14: 2141001.
180. Ramírez-Elías MG, González FJ. Raman spectroscopy for *in vivo* medical diagnosis. Raman Spectrosc. 2018; 293.
181. Hirsch M, Wareham RJ, Martin-Fernandez ML, Hobson MP, Rolfe DJ. A stochastic model for electron multiplication charge-coupled devices–from theory to practice. PloS one. 2013; 8: e53671.
182. Smulko J, Wróbel MS, Barman I. Noise in biological raman spectroscopy. IEEE. p. 1-6.
183. Jahn I, Grjasnow A, John H, Weber K, Popp J, Hauswald W. Noise Sources and Requirements for Confocal Raman Spectrometers in Biosensor Applications. Sensors. 2021; 21: 5067.
184. Zhao X, Liu G, Sui Y, Xu M, Tong L. Denoising method for Raman spectra with low signal-to-noise ratio based on feature extraction. Spectrochimica Acta Part a-Molecular and Biomolecular Spectroscopy. 2021; 250: 119374.
185. Clupek M, Matejka P, Volka K. Noise reduction in Raman spectra: Finite impulse response filtration versus Savitzky-Golay smoothing. Journal of Raman Spectroscopy. 2007; 38: 1174-9.
186. Gebrekidan M, Knipfer C, Braeuer A. Vector casting for noise reduction. Journal of Raman Spectroscopy. 2020; 51: 731-43.
187. Fan X, Zeng Y, Zhi Y, Nie T, Xu Y, Wang X. Signal-to-noise ratio enhancement for Raman spectra based on optimized Raman spectrometer and convolutional denoising autoencoder. Journal of Raman Spectroscopy. 2021; 52: 890-900.
188. Barton S, Ward T, Hennelly B. Algorithm for optimal denoising of Raman spectra. Analytical Methods. 2018; 10: 3759-69.
189. Kerr L, Byrne H, Hennelly B. Optimal choice of sample substrate and laser wavelength for Raman spectroscopic analysis of biological specimen. Analytical Methods. 2015; 7: 5041-52.
190. Strobbia P, Cupil-Garcia V, Crawford B, Fales A, Pfefer T, Liu Y, et al. Accurate *in vivo* tumor detection using plasmonic-enhanced shifted-excitation Raman difference spectroscopy (SERDS). Theranostics. 2021; 11: 4090-102.
191. Cordero E, Korinth F, Stiebing C, Krafft C, Schie I, Popp J. Evaluation of Shifted Excitation Raman Difference Spectroscopy and Comparison to Computational Background Correction Methods Applied to Biochemical Raman Spectra. Sensors. 2017; 17: 1724.
192. Gebrekidan M, Knipfer C, Stelzle F, Popp J, Will S, Braeuer A. A shifted-excitation Raman difference spectroscopy (SERDS) evaluation strategy for the efficient isolation of Raman spectra from extreme fluorescence interference. Journal of Raman Spectroscopy. 2016; 47: 198-209.
193. Wei D, Chen S, Liu Q. Review of Fluorescence Suppression Techniques in Raman Spectroscopy. Applied Spectroscopy Reviews. 2015; 50: 387-406.
194. Guo S, Popp J, Bocklitz T. Chemometric analysis in Raman spectroscopy from experimental design to machine learning-based modeling. Nature Protocols. 2021; 16: 5426-59.
195. Siddhanta S, Wrobel M, Barman I. Integration of protein tethering in a rapid and label-free SERS screening platform for drugs of abuse. Chemical Communications. 2016; 52: 9016-9.
196. Sha M, Xu H, Penn S, Cromer R. SERS nanoparticles: a new optical detection modality for cancer diagnosis. Nanomedicine. 2007; 2: 725-34.
197. Langer J, de Aberasturi D, Aizpurua J, Alvarez-Puebla R, Auguie B, Baumberg J, et al. Present and Future of Surface-Enhanced Raman Scattering. ACS Nano. 2020; 14: 28-117.
198. Ganguly P, Breen A, Pillai S. Toxicity of Nanomaterials: Exposure, Pathways, Assessment, and Recent Advances. ACS Biomaterials Science & Engineering. 2018; 4: 2237-75.
199. Yan L, Gu Z, Zhao Y. Chemical Mechanisms of the Toxicological Properties of Nanomaterials: Generation of Intracellular Reactive Oxygen Species. Chemistry-an Asian Journal. 2013; 8: 2342-53.
200. Hull M, Kennedy A, Steevens J, Bednar A, Weiss C, Vikesland P. Release of Metal Impurities from Carbon Nanomaterials Influences Aquatic Toxicity. Environmental Science & Technology. 2009; 43: 4169-74.